

Exhumation of ultrahigh-pressure rocks beneath the Hornelen segment of the Nordfjord-Sogn Detachment Zone, western Norway

Scott Johnston
Bradley R. Hacker

Department of Earth Science, University of California, Santa Barbara, CA 93106-9630, USA

Mihai N. Ducea

Department of Geosciences, University of Arizona, Gould-Simpson Building #77, 1040 E 4th St., Tucson, AZ 85721, USA

ABSTRACT

The Nordfjord-Sogn Detachment Zone of western Norway represents an archetype for crustal-scale normal faults that are typically cited as one of the primary mechanisms responsible for the exhumation of ultrahigh-pressure (UHP) terranes. In this paper, we investigate the role of normal-sense shear zones with respect to UHP exhumation using structural geology, thermobarometry, and geochronology of the Hornelen segment of the Nordfjord-Sogn Detachment Zone. The Hornelen segment of the zone is a 2–6 km thick, top-W shear zone, primarily developed within amphibolite-grade allochthonous rocks, that juxtaposes the UHP rocks of the Western Gneiss Complex in its footwall with lower-grade allochthons and Carboniferous-Devonian Basins in its hanging wall. New thermobarometry and Sm/Nd garnet geochronology show that these top-W fabrics were initiated at lower crustal depths of 30–40 km between 410 Ma and 400 Ma. Structural geology and quartz petrofabrics indicate that top-W shear was initially relatively evenly distributed across the shear zone, and then overprinted by discrete ductile-brittle detachment faults at slower strain rates during progressive deformation and exhumation. These results require a three-stage model for UHP exhumation in which normal-sense shear zones exhumed UHP rocks from the base of the crust along initially broad ductile shear zones that were progressively overprinted by discrete ductile-brittle structures.

Keywords: ultrahigh-pressure rocks, exhumation, Nordfjord-Sogn Detachment Zone, low-angle detachment, western Norway, Hornelen Region.

INTRODUCTION

Ultrahigh-pressure (UHP) terranes—which range from km-scale nappes to tens-of-thousands-of-square-kilometer provinces—experience rapid and near-isothermal decompression from metamorphic conditions within the coesite stability field (>~27 kbar) to the upper crust at plate-tectonic rates exceeding 10 mm/yr (e.g., Baldwin et al., 2004; Glodny et al., 2005; Root et al., 2005; Parrish et al., 2006). To explain these impressive exhumation rates, a variety of kinematic models have been employed that incorporate one or a combination of exhumation mechanisms that include: wedge extrusion (e.g., Chemenda et al., 2000), channel flow (e.g., Beaumont et al., 2001), subhorizontal coaxial thinning followed by non-coaxial removal of the upper crust (e.g., Dewey et al., 1993), and normal-sense reactivation of the suture zone (e.g., Hacker et al., 2003). While all of these models cite normal-sense shear zones along the upper contact of the exhuming UHP terrane, the amount of offset and the tectonic setting in which the normal-sense displacement occurred vary drastically in the different models. These differences in the style of normal-sense shearing have important geologic implications beyond the exhumation of UHP rocks, representing an essential step toward a better understanding of first-order plate-tectonic processes as far reaching as the kinematic evolution of continental collision and orogeny, the formation and composition of the lower continental crust, melt generation, the geometry and depositional patterns of syn-orogenic basins, and the forces driving plate motion.

We present a case study from western Norway that places important constraints on the style of normal-sense shearing associated with UHP exhumation. The size and excellent exposures of the Norwegian (U)HP (high-pressure/

ultrahigh-pressure) provinces, a lack of post-orogenic deformation, and the preservation of original tectonostratigraphic contacts between the (U)HP provinces with structurally higher tectonostratigraphic units, provide a unique opportunity to reconstruct the history of an UHP orogen and characterize UHP exhumation. The Norwegian (U)HP provinces are thought to have been primarily exhumed by the Nordfjord-Sogn Detachment Zone, a major top-W shear zone that extends >100 km along orogenic strike (Milnes et al., 1997; Andersen, 1998; Labrousse et al., 2004). This quantitative study focuses on the Hornelen segment of the Nordfjord-Sogn Detachment Zone to address a specific set of questions designed to characterize deformation related to normal-sense displacement above UHP terranes: (1) using structural geology and electron back-scatter diffraction on quartzites, we determine how strain was partitioned within the shear zone and across tectonostratigraphic contacts; (2) using thermobarometry, we quantify the depth from which different tectonostratigraphic units were exhumed and the depth at which normal-sense shear initiated; and (3) using Sm/Nd garnet geochronology, we constrain the timing of normal-sense displacement with respect to (U)HP metamorphism. Ultimately, our results are used to investigate models for (U)HP exhumation and quantify the component of UHP exhumation accomplished through normal-sense shear.

GEOLOGIC SETTING

The Scandinavian Caledonides formed through a series of orogenic events associated with the closure of the Iapetus Ocean during the Ordovician-Devonian, and culminated with the emplacement of the Caledonian nappe stack and the formation of the Norwegian UHP provinces as Baltica and Laurentia collided (Roberts and

Sturt, 1980; Cuthbert et al., 1983; Gee et al., 1985; Hacker and Gans, 2005). The Caledonian nappe stack, best preserved in the foreland of eastern Norway and Sweden, consists of a series of tectonostratigraphic units (Fig. 1): fragments of Laurentia in the Uppermost Allochthon; ophiolitic mélanges, ocean-margin sediments, and outboard Baltica terranes in the Upper Allochthon; and imbricated basement-cover sequences representing distal regions of the Baltica margin in the Middle and Lower Allochthons (Gee et al., 1985; Roberts and Gee, 1985). These nappes were thrust southeastward >200 km over the Proterozoic granodioritic-granitic gneisses of the Western Gneiss Complex, correlative to the (par)-autochthonous Baltica basement, in a series of events that initiated as early as the Wenlockian (ca. 425 Ma, Andersen et al., 1990), and continued through 415–408 Ma in the Upper and Middle Allochthons (Fossen and Dunlap, 1998; Hacker and Gans, 2005). Peak

metamorphic conditions in these basement gneisses range from upper-amphibolite facies in the east near the foreland (Walsh and Hacker, 2004), through UHP coesite-eclogite facies in the west (Smith, 1984; Wain, 1997). The felsic gneisses of the Western Gneiss Complex include outcrop- to km-scale eclogite boudins that record northwestward increasing P-T conditions (Krogh, 1977; Carswell and Cuthbert, 2003), suggesting subduction of Baltica beneath Laurentia up to UHP depths by 415–400 Ma (Krogh and Carswell, 1995; Carswell and Cuthbert, 2003; Root et al., 2004; Kylander-Clark et al., 2007). The Western Gneiss Complex is overlain by complexly infolded orthogneisses and paragneisses correlated with the structurally higher allochthons (Robinson, 1995). Eclogite boudins within these allochthons suggest that the allochthons were also involved in the Late-Caledonian UHP event (Terry et al., 2000; Root et al., 2005; Young, 2005).

Following continental subduction and UHP metamorphism, the Caledonides were reshaped by a major extensional event that rapidly exhumed rocks from lower crustal and mantle depths into the upper crust. In the foreland, this extension was accommodated through top-W reactivation of older top-SE contractional detachments, and the nappe stack was exhumed through muscovite closure to Ar by ca. 400 Ma (Fossen and Dunlap, 1998). In the hinterland, muscovite cooling ages become progressively younger westward and down section from 400 Ma at higher structural levels in the east to 380 Ma in the westernmost UHP provinces (Root et al., 2005; Walsh et al., 2007). Most of this exhumation is thought to have occurred through top-W, normal-sense displacement along a series of detachments that crop out along the west coast of Norway, combined with non-coaxial normal-sense shear and vertical thinning in the detachment footwalls (Andersen

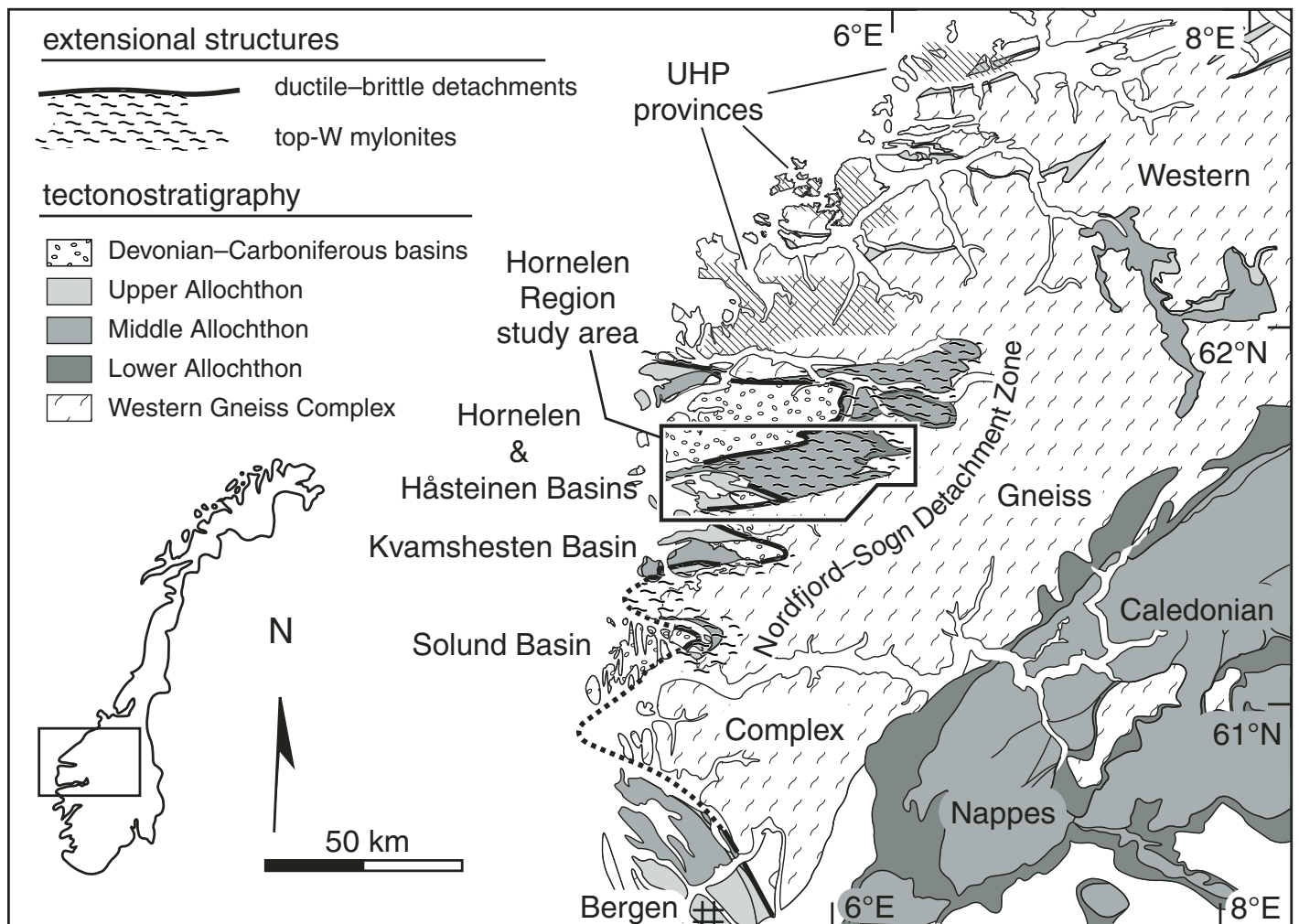


Figure 1. Regional map of the Norwegian Caledonides showing the relative location of the Caledonian nappe stack, the Western Gneiss Complex, the Devonian basins, and the Nordfjord-Sogn Detachment Zone.

and Jamtveit, 1990; Milnes et al., 1997; Andersen, 1998; Fossen and Dunlap, 1998). Of these extensional detachments, the Nordfjord-Sogn Detachment Zone is the largest and best exposed, stretching ~100 km from Sognefjord to Nordfjord (Fig. 1, Norton, 1987).

The Nordfjord-Sogn Detachment Zone is a 2- to 6-km-thick shear zone with pervasively developed amphibolite-greenschist facies asymmetric shear structures that fade down section into predominantly symmetric extensional fabrics (Andersen and Jamtveit, 1990; Dewey et al., 1993; Andersen et al., 1994; Wilks and Cuthbert, 1994; Johnston et al., 2007). This late-Caledonian extension was accompanied by Devonian-Carboniferous deposition of coarse conglomerates and sandstones in a series of extensional basins (Norton, 1987; Eide et al., 2005). During progressive exhumation and cooling, the early ductile extensional fabrics of the Nordfjord-Sogn Detachment Zone were overprinted and at least partially excised by discrete ductile-brittle detachments (Braathen, 1999; Braathen et al., 2004). Deformation continued along these detachments through the Late Permian and was reactivated in the Jurassic-Cretaceous (Eide et al., 1997) but represents only the final component of deformation responsible for the astounding juxtaposition of footwall UHP eclogites with low greenschist-grade, hanging-wall Devonian-Carboniferous sediments across the shear zone (Osmundsen et al., 1998; Braathen et al., 2004).

The Hornelen segment of the Nordfjord-Sogn Detachment Zone, underlying the Håsteinen and Hornelen Basins, includes the longest and broadest continuous segment of the zone, and the most complete exposures of allochthonous rocks in western Norway (Fig. 2). These relationships make it ideal for investigating the mechanics of deformation within the shear zone and the nature of the contacts between the (U)HP Western Gneiss Complex and its overlying, lower pressure allochthons. Noting significant structural omission beneath the Hornelen Basin, the extensional nature of the low-angle detachment surfaces was first recognized by Hossack (1984), who suggested that the detachment surfaces represent listric normal faults responsible for opening the Devonian-Carboniferous basins. This model was developed further by subsequent authors who defined the Nordfjord-Sogn Detachment Zone and recognized that significant extensional displacement also occurred within the multiple-km-thick packages of top-W mylonites and asymmetric fabrics located in the allochthons and upper levels of the Western Gneiss Complex immediately beneath the detachment surfaces (Norton, 1987; Séranne and Séguret, 1987; Andersen and Jamtveit, 1990; Dewey et al., 1993; Andersen et al., 1994; Wilks

and Cuthbert, 1994; Krabbendam and Dewey, 1998). This previous body of work lays the conceptual foundation for the present quantitative study of the strain partitioning, metamorphic conditions, and timing within the Hornelen segment of the Nordfjord-Sogn Detachment Zone.

HORNELEN REGION TECTONOSTRATIGRAPHY

The tectonostratigraphy of the Hornelen Region was described by Bryhni and Grimstad (1970) and mapped by Bryhni and Lutro (Bryhni, 2000; Bryhni and Lutro, 2000b, 2000a, 2000c; Lutro and Bryhni, 2000). From the bottom up, the Hornelen Region tectonostratigraphy includes the Western Gneiss Complex, the Svartekari Group, the Eikefjord and Lykkjebø Groups, and the Sunnarvik Group, which are loosely correlated with regional nappe stack tectonostratigraphy: Baltica basement, the Lower Allochthon, the Middle Allochthon, and the Upper Allochthon, respectively (Fig. 2). These rocks are in fault contact with, and unconformably overlain by, the Devonian-Carboniferous sediments of the Hornelen and Håsteinen Basins that define the top of the tectonostratigraphic section.

The Western Gneiss Complex is the lowermost tectonostratigraphic unit exposed within the Hornelen Region. In contrast to the wide variety of rock types found in the overlying units, the Western Gneiss Complex consists of relatively monolithologic Precambrian orthogneisses that range from granite-granodiorite with local 1- to 2-cm K-feldspar augen, to relatively undeformed quartz monzonite with abundant 2- to 3-cm K-feldspar augen. In contrast to the amphibolite-facies conditions preserved within these felsic orthogneisses, outcrop- to km-scale mafic boudins preserve older eclogitic assemblages that, along Nordfjord, range from UHP in the west to HP in the east (e.g., Cuthbert et al., 2000; Young et al., 2007). The foliation within the host gneiss is cut by abundant, pegmatitic granitic to syenitic dikes. In the several hundred meters below the contact with the overlying allochthons, these dikes become increasingly deformed and transposed into the foliation, and symmetric fabrics are progressively replaced by asymmetric fabrics.

The Western Gneiss Complex is overlain by metamorphosed Precambrian plutonic and sedimentary rocks of the Svartekari Group. The lowermost unit within the Svartekari Group consists of <100 m of interlayered coarse muscovite schists, marbles, quartzites, and rare quartz-pebble conglomerates. This paragneiss sequence is overlain by up to 1000 m of muscovite-rich orthogneisses with abundant

cross-cutting quartz dioritic-granitic dikes and lenses, and local amphibolite bodies up to 200 m in length. These cross-cutting dikes are variably transposed into the foliation, many forming asymmetric boudins; top-W shear-sense indicators are pervasively developed throughout the Svartekari Group. The Svartekari Group orthogneisses are correlated with the Lower Allochthon, whereas the structurally lower Svartekari Group paragneisses may represent an overturned section of depositional cover to the orthogneisses, or alternatively, could be part of the cover sequences unconformably overlying the Baltica autochthon.

The Eikefjord Group orthogneisses and the Lykkjebø Group paragneisses, which overlie the Svartekari Group, are considered to be a basement-cover pair within the Middle Allochthon. The Eikefjord Group consists of (1) dark, alkalic, massive to banded, fine-grained, biotite-K-feldspar gneisses with common outcrop-to km-scale boudins of anorthosite, and rare garnet-amphibolite and garnet-anorthosite bodies; and (2) granitic augen gneisses and megacrystic augen gneisses variably altered to biotite-rich, albite-porphyroblast schists. The Lykkjebø Group consists primarily of feldspathic quartzites with minor interlayers of muscovite schist, rare pebble conglomerates, and a distinctive, coarse, garnet-muscovite schist found along contacts with the Eikefjord Group. This garnet-muscovite schist in the Lykkjebø Group immediately below and above the Eikefjord Group suggests at least three structural repetitions of individual basement-cover units, and an inverted lower limb to the nappe. Subsequent to nappe emplacement, both the Eikefjord and Lykkjebø Groups were strongly affected by regional extension and carry a foliation characterized by pervasive top-W shear fabrics.

The Sunnarvik Group, correlated with the Solund-Stavfjord ophiolite of the Upper Allochthon, structurally overlies the Eikefjord and Lykkjebø Groups. Consisting primarily of metavolcanic rocks overlain by a thin veneer of feldspathic quartzites and muscovite schists, the Sunnarvik Group is intruded by granodioritic to keratophytic igneous rocks, and is characterized by a greenschist-facies foliation that generally lacks ductile asymmetric shear fabrics.

The Håsteinen and western Hornelen Basins rest unconformably on the Sunnarvik Group, whereas the northern, eastern, and western margins of the Hornelen Basin are in fault contact with the Eikefjord and Lykkjebø Groups. Sedimentary facies within the Hornelen Basin vary from proximal conglomerates near the basin margins, to sandstones and distal shales in the interior of the basin (Steel et al., 1985), suggesting that these basins formed as isolated

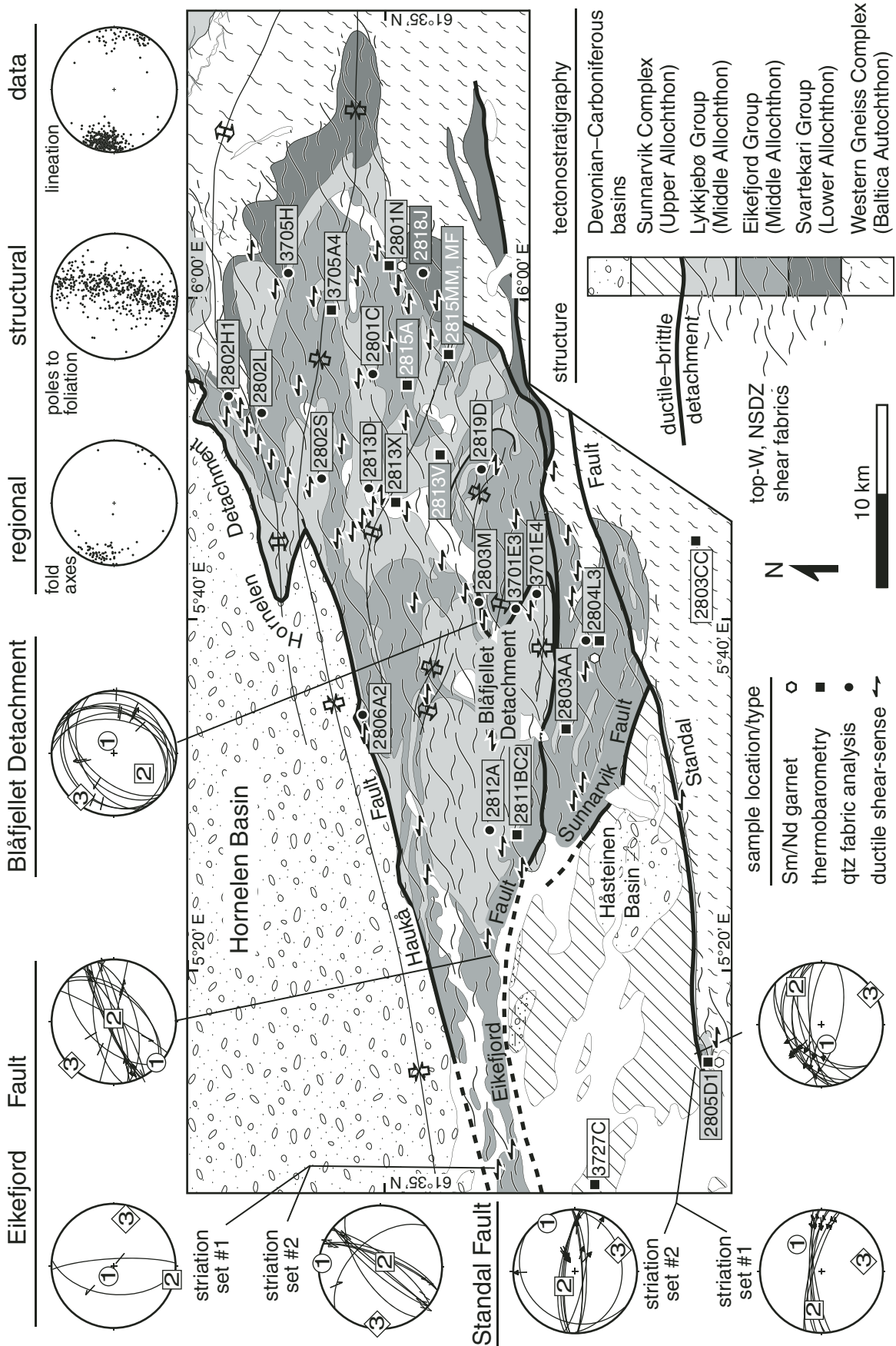


Figure 2. Geologic map of the Hornelen Region (based on mapping by Bryhni and Lutro, 2000a, 2000b, 2000c; this study) showing sample locations, major ductile-brittle faults, extent of top-W Nordfjord-Sogn Detachment Zone shear fabrics, and structural data. All stereograms are lower hemisphere, equal-area plots. Fault-slip data are plotted with fault-plane orientations indicated by great circles, striations indicated by arrows illustrating slip direction, and principal stress axes determined through stress inversion indicated by points labeled 1–3.

basins. Clast studies (Cuthbert, 1991), together with 1700–1600 Ma, 1000 Ma, and Ordovician detrital zircon populations (Johnston et al., 2003; Johnston, 2006), suggest sourcing from the Sunnarvik, Eikefjord, and Lykkjebø Groups. Bedding within the Hornelen sedimentary rocks dips consistently 10–30° E across the length of the basin, yet despite this tilting and exaggerated stratigraphic thickness, the Hornelen Basin is apparently unaffected by either syn- or post-depositional faults of significant offset, and reached only low greenschist-facies conditions (Norton, 1987).

STRUCTURAL GEOLOGY

The rocks of the Hornelen Region have complicated, polygenetic deformational histories with overprinting structures that formed sequentially during E-W Caledonian contraction and extension, followed by Late Devonian through Early Carboniferous N-S contraction, and multiple episodes of E-W extension active into the Permian (e.g., Braathen, 1999). Although the microfibrils and original orientation of structures formed during Caledonian contraction have been altered by subsequent deformation, remnants of the Caledonian contraction are preserved in isoclinal folds that repeat the tectonostratigraphic section throughout the study area. The folds are most easily seen at the outcrop scale within the Lykkjebø Group quartzites, and have axes that trend WNW and axial planes that are subparallel to the foliation. Locally, these folds are associated with a weak axial planar cleavage defined by minor growth and bending of micaceous minerals. At the map scale, the tectonostratigraphic contacts between the Lykkjebø and Eikefjord Groups are also isoclinally folded (Fig. 3A), and the repetition of the Lykkjebø Group above and below the Eikefjord Group (Fig. 2) suggests significant thickening of the local tectonostratigraphy, and that the Middle Allochthon regional geometry may be an overturned anticline.

During Caledonian exhumation, these early contractional structures were strongly overprinted by E-W extension and top-W shear fabrics that define the Nordfjord-Sogn Detachment Zone. In the Western Gneiss Complex, Svartekari, Eikefjord, and Lykkjebø Groups, this extensional deformation is characterized by the development of a pervasive WNW-ESE stretching lineation that is defined by biotite, quartz ribbons, and amphibole that either formed or rotated into the stretching direction (Fig. 2). Although symmetric fabrics dominate the bulk of the Western Gneiss Complex, the asymmetric shear fabrics of the Nordfjord-Sogn Detachment Zone become increasingly prominent in the 500–1000 m below

the contact with the overlying allochthons, and are pervasively developed throughout the Svartekari, Eikefjord, and Lykkjebø Groups in a 2- to 6-km-thick shear zone. Asymmetric structures within the Nordfjord-Sogn Detachment Zone include S-C fabrics, sigma and delta clasts, shear bands (extension crenulation cleavage), and asymmetric boudinage, and yield consistently top-WNW sense of shear (Fig. 3B, C). The Nordfjord-Sogn Detachment Zone is also characterized by a series of discrete ductile-brittle, low-angle detachments, also, with top-W displacement, that reactivated and cut the high-temperature asymmetric shear fabrics. The uppermost of these low-angle detachments, and high-angle, E-W striking strike-slip and normal faults juxtapose the top-W fabrics of the Nordfjord-Sogn Detachment Zone with the Sunnarvik Group and the Devonian-Carboniferous basins. Consistent E-W lineations are not found in the Sunnarvik Group or the Devonian-Carboniferous basins, indicating that ductile stretching during Caledonian extension was limited to rocks below the Upper Allochthon.

Quartz Lattice-Preferred Orientations in High-Temperature Rocks

To better understand deformation history, strain partitioning, and variability within the Nordfjord-Sogn Detachment Zone, quartz microfibrils were analyzed from sixteen Lykkjebø Group quartzites at different tectonostratigraphic levels throughout the shear zone (Table 1). Lykkjebø Group quartzites are arkosic, containing 20–40% feldspar and up to 10% muscovite. Petrographic observations reveal that feldspar is typically weakly deformed, with local undulatory extinction, minor subgrain development, and late brittle fractures. Quartz is dynamically recrystallized in all samples, and textures (Hirth and Tullis, 1992; Stipp et al., 2002b) reveal that the dominant recovery mechanism changed from subgrain rotation (SGR, typified by quartz ribbons and core-and-mantle structures) at higher structural levels to grain-boundary migration (GBM, typified by irregular grain shapes with ‘island grains’ and lobate grain boundaries) in the lowermost quartzite unit (Fig. 3D, E, F). Top-W shear fabrics—including mica-fish, shear bands, and S-C fabrics (Fig. 3D, E, F)—were observed in ten of the analyzed samples, with the remaining six displaying either indistinct or symmetric shear fabrics; top-E microstructures were not observed in any of the quartzite thin sections.

Quartz lattice-preferred orientations (LPOs) were measured from quartz-rich areas of the samples using electron-backscatter diffraction (EBSD). Because the normal to the lattice-slip plane rotates toward the shear plane

and the lattice-slip direction rotates toward the shear direction during progressive deformation, LPOs can be used to investigate shear symmetry, qualitatively assess constrictional-flattening strain, and determine active slip systems (Schmid and Casey, 1986). Diffraction patterns were collected on 1.4 × 1-mm grids with a 5-μm step size, using a JEOL 6300 scanning electron microscope coupled with an HKL Nordlys camera. CHANNEL 5 HKL software was used to index the diffraction patterns, create crystal orientation maps, and ultimately define and characterize individual quartz grains by locating grain boundaries (identified where lattice misorientations exceed 10°). LPOs generated from crystal orientation maps were checked to ensure that they were representative of the entire thin section by creating secondary LPOs from diffraction patterns collected on cm-scale grids with step sizes much greater than the grain size.

All the quartzite samples examined by EBSD yielded strong LPOs with peak c-axis concentrations ≥3 times mean uniform distribution (Fig. 4). Top-W LPO asymmetry, distinguished by c- and a-axis patterns that are rotated counterclockwise with respect to the principal strain axes, is observed in thirteen of sixteen samples and is indicative of simple shear. These LPO results support top-W shear in seven samples that exhibit top-W petrographic microstructures and suggest that top-W shear was also important in six samples that do not contain petrographically distinct asymmetry. Top-E LPO asymmetry, observed in three samples that contain clear top-W shear bands, may be the result of perturbations in the flow field creating local top-E displacement within the thin section, back rotation of foliation due to well-developed shear bands, or variations in the ages of the thin-section textures relative to the quartz LPOs. The LPOs from the structurally high quartzites yield c-axis girdles compatible with a combination of (c)<a>, {r}<a>, and {m}<a> slip, and are distinct from LPOs in the lowermost quartzites that display c-axis maxima near the Y direction that are compatible with {m}<a> slip (Fig. 4A, B). This change from c-axis girdles to single c-axis maxima is consistent with the previously discussed petrographic observations that indicate a change in recovery mechanism from subgrain rotation to grain-boundary migration (Stipp et al., 2002b) from higher to lower structural levels within the Lykkjebø Group quartzites. A-axis patterns at all structural levels and regardless of shear-sense (Fig. 4) form maxima near the X direction, and minima that plot in the X-Z plane, or in the case where only (c)<a> slip is observed, in the X-Y plane. As opposed to constrictional strain, which forms small circles near the X direction, or flattening strain, which forms

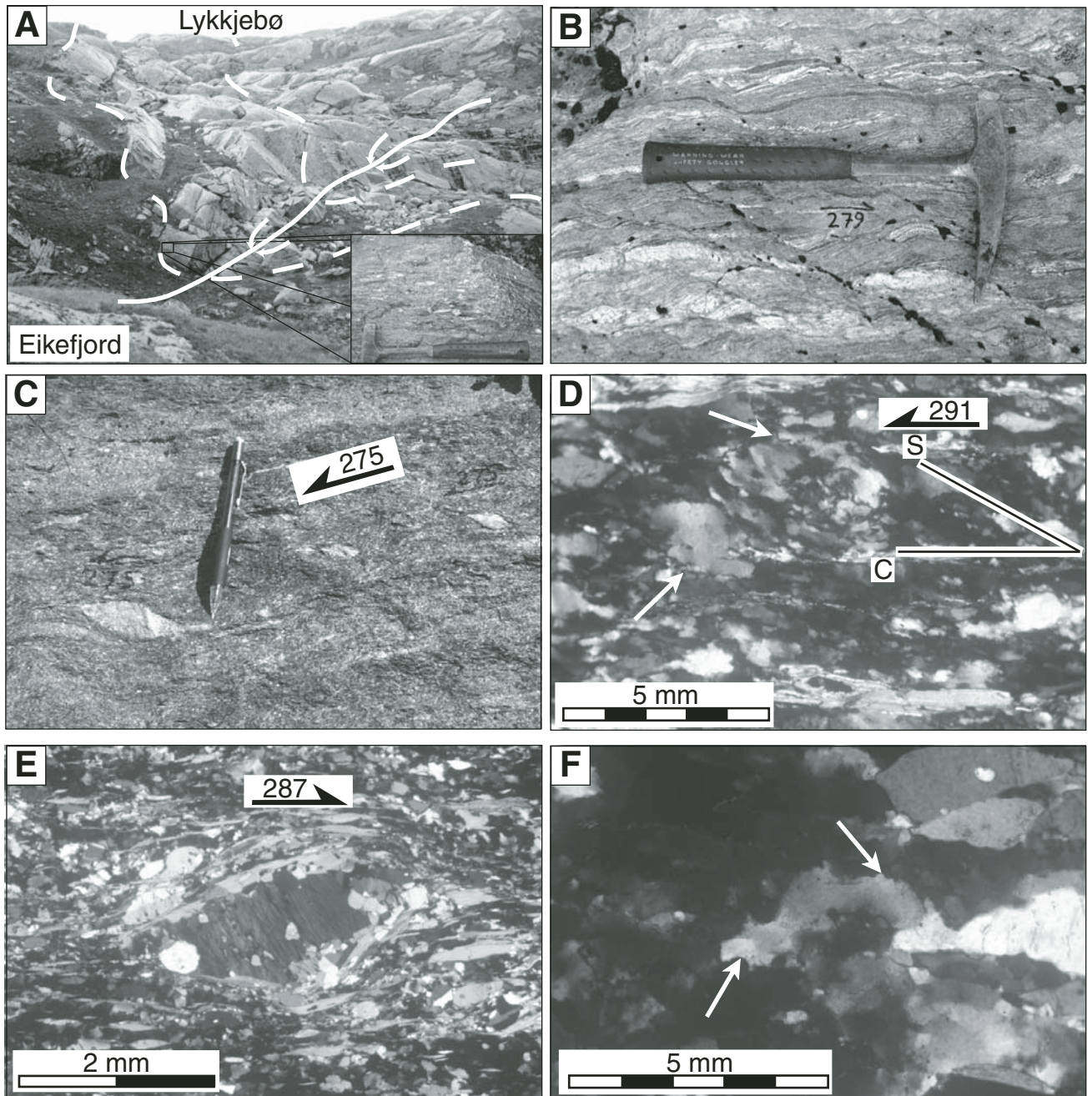


Figure 3. (A-C) Outcrop structures: (A) Overturned folding of the contact between the Eikefjord Group and the Lykkjebø Group, here shown with an upside-down basal conglomerate. (B) Penetrative shear bands in the Eikefjord Group indicating top-W (toward 279°) sense of shear. (C) Feldspar sigma clasts indicating top-W (275°) sense of shear in the Eikefjord Group. (D-F) Microstructures: (D) Quartzite sample 2806A2 from structurally high levels of the Lykkjebø Group showing top-W S-C fabrics and recrystallized grains mantling larger grains (white arrows) indicative of subgrain-rotation recovery. (E) Top-W, recrystallized feldspar sigma clast in quartzite sample 2804L31 from low structural levels of the Lykkjebø Group. (F) Detail of 284L31 showing lobate quartz grain boundaries indicative of grain-boundary migration recovery.

TABLE 1. MICROSTRUCTURAL DATA AND PIEZOMETRY FROM THE LYKKJEBØ GROUP QUARTZITES

Sample	Structural level	Petrographic observations		EBSD observations				Piezometry	
		Deformation mechanism	Symmetry	Slip plane	D (µm)	± [†]	Symm.	σ _g (MPa) [‡]	τ (MPa) [‡]
3701E3	D-B fault	SGR	top-W	a, r & m	25.5	2.2	top-W	74.7	37.4
3701E4	D-B fault	SGR	top-W	a, r & m	25.3	2.2	top-W	75.2	37.6
2819D	high	SGR/GBM	top-W	a, r & m	64.8	3.5	top-E	39.6	19.8
2805S [§]	high	SGR	top-W	r & m			top-W		
2813D	high	BLG II	symmetric	a	38.5	3.0	top-W	56.5	28.2
3628D	high	SGR	no clear	r & a	39.3	3.0	top-W	55.7	27.9
2806A2	high	SGR	top-W	r & m	39.8	2.5	top-W	55.2	27.6
2802S	high	SGR	symmetric	a, r & m	38.0	2.6	top-W	56.9	28.5
2803M	high	SGR/GBM	top-W	a, r & m	38.4	2.6	top-W	56.6	28.3
2801C	high	BLG/SGR	symmetric	a, r & m	40.3	2.6	top-W	54.8	27.4
2812A	high	SGR	symmetric	a, r & m	40.7	2.5	top-W	54.4	27.2
3630D	high	GBM	top-W	m	42.8	2.7	top-W	52.5	26.3
2802H1	low	GBM	top-W	m	40.2	2.8	top-W	54.8	27.4
2802L	low	GBM	top-W	m	42.1	2.7	top-W	53.1	26.6
3705H	low	GBM	symmetric	m	48.3	3.0	top-W	48.4	24.2
2804L31	low	GBM	top-W	m	55.3	1.7	top-W	44.2	22.1
2818J	low	SGR	top-W	r & m	38.2	2.8	top-E	56.8	28.4
2804L2	low	GBM	top-W	m	41.3	1.7	top-E	53.8	26.9
D-B fault avg. [#]					25.4	2.2		74.4 ^{+5.3} _{-3.5}	37.2 ^{+2.7} _{-1.8}
high avg. [#]					39.7	1.8		55.2 ^{+1.9} _{-1.5}	27.6 ^{+0.9} _{-0.8}
low avg. [#]					46.7	7.5		48.3 ^{+7.9} _{-3.7}	24.1 ^{+3.9} _{-1.9}

Note: Abbreviations: D—grain diameter; D-B fault—ductile-brittle fault; high avg.—average of structurally high top-W samples; low avg.—average of structurally low top-W samples.

[†]1σ.

[‡]σ_g is calculated after Twiss (1977, 1980); τ, maximum shear stress, = 0.5* σ_g.

[§]Grain size data, and thus stress and strain rate, were not calculated for 2805S due to poor coverage of crystal orientation map.

[#]2819D, 2818J, and 2804L2 were not used in average calculations for high and low structural levels because they have top-E LPO asymmetry. Average grain size estimates are weighted averages; reported stress estimates are population mode and 1 sigma errors derived through Monte Carlo simulations propagating grain size errors only.

small circles near the Y direction, these a-axis patterns are generally indicative of plane strain (Schmid and Casey, 1986).

Geometric mean-grain diameters, also measured from EBSD crystal-orientation maps, were applied to grain-size piezometers to determine stress variations across the Nordfjord-Sogn Detachment Zone (Table 1). The grain diameter in samples with clear top-W LPO asymmetry increases slightly from 39.7 ± 1.8 µm at higher structural levels to 46.7 ± 7.5 µm in the lowest level of the Lykkjebø Group quartzites; these populations are significantly different at the 95% confidence level according to Student's t-test. Applying the grain-size piezometer of Twiss (1977; 1980)—as recommended by Stipp et al. (2002a)—yields maximum shear stresses of ~28 MPa and ~24 MPa for structurally higher and lower Lykkjebø Group quartzites, respectively.

Late Ductile-Brittle Deformation

Subsequent to this high-temperature ductile deformation, the asymmetric fabrics of the Nordfjord-Sogn Detachment Zone were cut by a series of discrete, low-angle ductile-brittle detachments that are characterized by dm-thick zones of top-W, fine-grained mylonites overprinted by brittle fault cores

with pseudotachylites and fault gouge. The largest of these structures, the Hornelen-Sunnarvik-Standal Detachment system, juxtaposes lower plate rocks with top-W ductile structures with upper plate rocks that lack top-W ductile structures, and defines the upper limit of the high-temperature asymmetric fabrics within the Nordfjord-Sogn Detachment Zone (Fig. 2). In contrast, similar low-angle structures in the footwall of the Hornelen-Sunnarvik-Standal Detachment system, such as the Blåfjellet Detachment, are discontinuous, accumulated less strain, and contain the high-temperature asymmetric fabrics of the Nordfjord-Sogn Detachment Zone in both footwall and hanging wall positions (Fig. 2). Fault-slip analysis using stress inversion techniques applied to fault planes, striations, and displacement indicators (e.g., Ratschbacher et al., 1994; Ratschbacher et al., 2003), on fault planes within and related to the Blåfjellet Detachment, indicates continued top-W displacement during the final stages of brittle motion along the Blåfjellet Detachment (Fig. 2). Paleomagnetic data and ⁴⁰Ar/³⁹Ar geochronology on gouges from the Dalsfjord Fault, a similar fault beneath the Kvamshesten Basin, indicate that these faults remained active through the Permian and Jurassic (Torsvik et al., 1992; Eide et al., 1997).

Two quartzite samples from the mylonite zone enclosing the low-angle Blåfjellet Detachment at the south end of Størfjorden yielded LPOs with c-axis girdles compatible with a combination of (c)<a>, {r}<a>, and {m}<a> slip and a-axis patterns indicative of plane strain (Fig. 4C). Whereas both samples exhibit top-W microstructures including mica fish and shear bands, and strong top-W LPO asymmetry is observed in sample 3701E3, the symmetric LPO of sample 3701E4 is most likely the result of foliation back-rotation during the formation of late, well-developed shear bands. A mean grain size of 25.4 ± 2.2 µm from these Blåfjellet Detachment samples implies maximum shear stresses of ~37 MPa.

These low-angle detachments are cut by E-W striking, high-angle normal and strike-slip faults (Braathen, 1999; this study). Fault-slip analysis of m-scale fault planes near the Eikefjord and Standal Faults indicates initial E-W stretching and vertical thinning strongly overprinted by E-W stretching and N-S shortening (Fig. 2). This analysis is consistent with early E-W to SE-NW stretching followed by late sinistral shear inferred for the E-W striking Eikefjord and Standal Faults. This late faulting was accompanied by regional folding of the entire tectonostratigraphy and resulted in a

Figure 4A

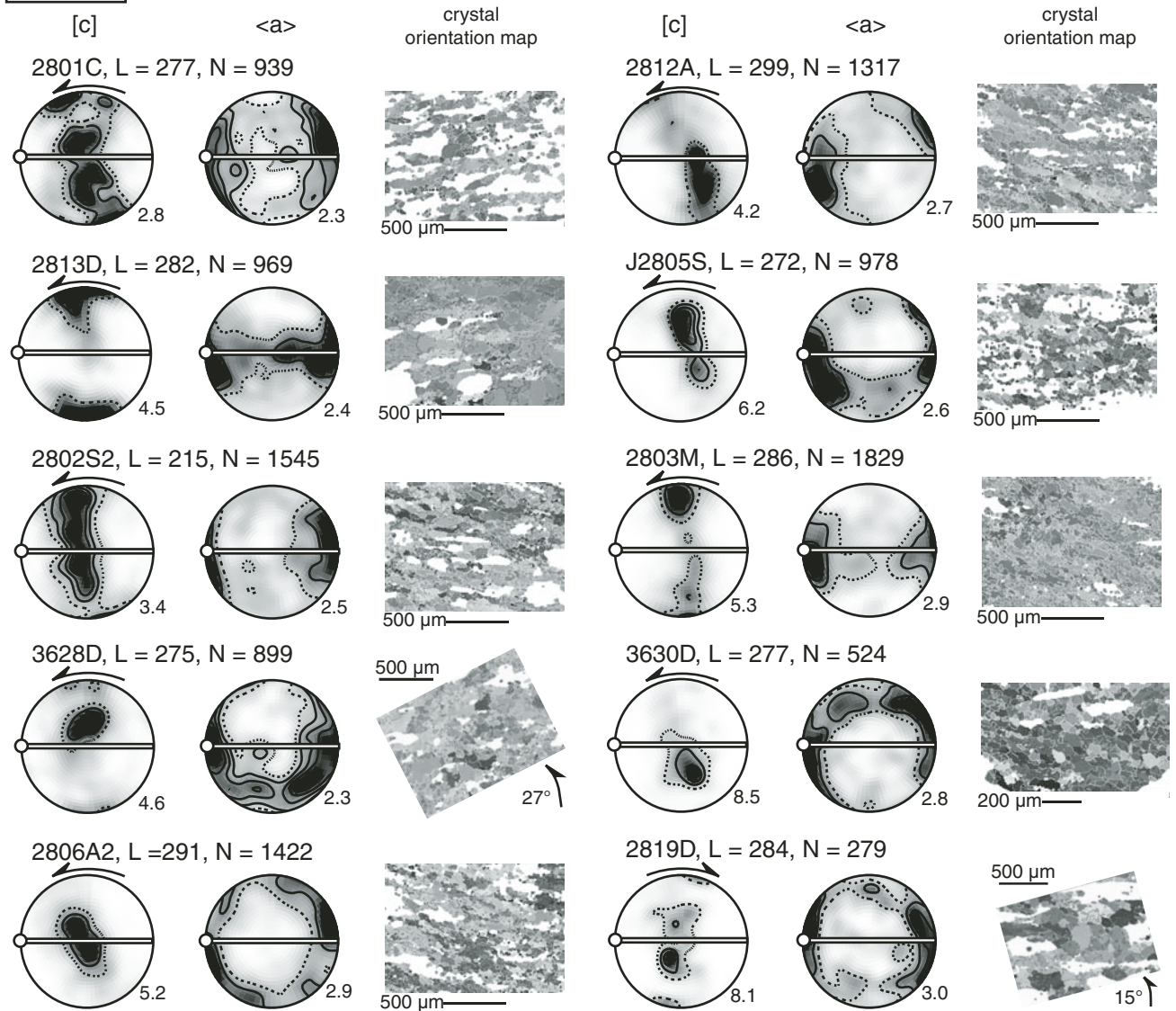


Figure 4. Lattice-preferred orientations and crystal orientation maps of the Lykkjebø Group quartzites from (A) higher structural levels, (continued on following page).

series of open, W-plunging anticlines and synclines with 5- to 10-km wavelengths (Fig. 2). Stratigraphic evidence from the Kvamshesten Basin indicates that deposition was synchronous with N-S contraction, and suggests that the Devonian-Carboniferous Basins were initially opened in a constrictional strain field (Chauvet and Séranne, 1994; Krabbendam and Dewey, 1998; Osmundsen et al., 1998). However, these broad folds also deform Hornelen Basin deposits, the Blåfjellet and Hornelen Detachments, as well as $^{40}\text{Ar}/^{39}\text{Ar}$ mica and K-feldspar age contours farther north in the Western Gneiss Complex, and indicate that at least some of this folding occurred in the upper crust

after 380 Ma, and possibly as late as 335 Ma (Root et al., 2005).

In summary, the new structural data provide several new results constraining the key structural events and styles of deformation in the Hornelen Region during the Caledonian. First, outcrop- to map-scale isoclinal folds within the allochthons likely produced during early Caledonian contraction are overprinted by top-W shear within the Nordfjord-Sogn Detachment Zone. Second, plane-strain top-W shear within the zone, restricted to the uppermost several hundred meters of the Western Gneiss Complex and the Svartekari, Eikefjord, and Lykkjebø Groups, is characterized by recovery mechanisms in

quartz that change from GBM at lower structural levels to SGR at higher structural levels, whereas maximum shear stresses were relatively constant at 24–28 MPa across the shear zone. Third, continued top-W displacement within the zone occurred along discrete ductile-brittle detachment faults with ductile envelopes characterized by SGR recovery mechanisms in quartz and elevated maximum shear stresses of 37 MPa, and brittle cores containing pseudotachylites and fault gouge. Finally, the top-W fabrics of the Nordfjord-Sogn Detachment Zone are cut by E-W striking strike-slip faults and folded into series of 5- to 10-km wavelength, W-plunging open folds.

Figure 4B

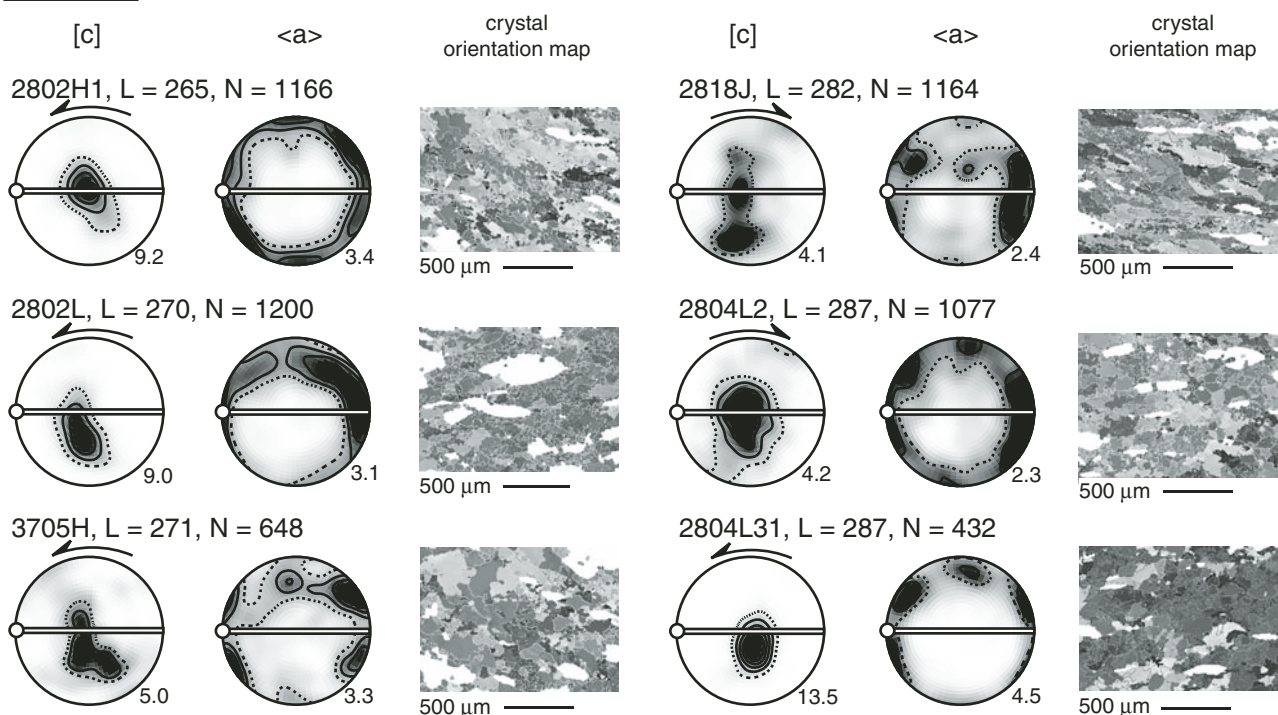


Figure 4C

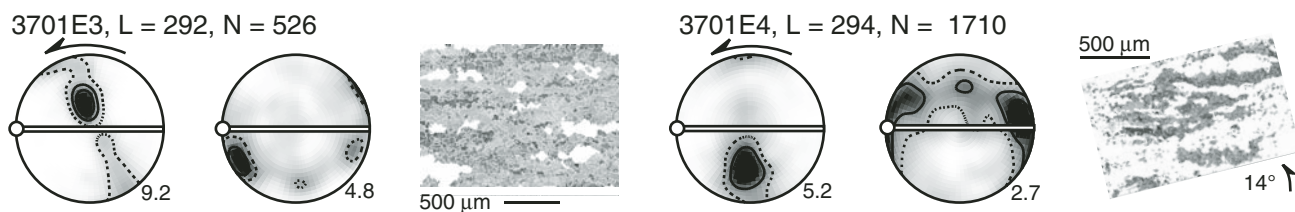


Figure 4 (continued). (B) lower structural levels, and (C) late ductile-brittle detachment faults. Following each sample name are the trend of the lineation (L =) and the number of oriented points (N =). Stereograms are lower hemisphere, equal-area plots with the sample foliation shown by a white line and lineation shown as a white dot. Contours indicate multiples of mean uniform distribution with the maximum value at the lower right of the stereogram. Shear-senses, indicated by arrows, were interpreted through consideration of the asymmetry for both c- and a-axis distributions. Grayscale coloring in crystal orientation maps reflects crystal orientation with respect to the sample surface.

METAMORPHIC PETROLOGY

Regional mapping and petrology in the Hornelen Region indicate that metamorphic grade increases down-section in a series of abrupt jumps across tectonostratigraphic contacts (e.g., Wilks and Cuthbert, 1994). The extent of these metamorphic breaks and the depths from which each tectonostratigraphic unit was exhumed were quantified with thermobarometry. Phase compositions were measured at University of California, Santa Barbara, on a Cameca SX-50 electron microprobe operated at 15 kV and 15 nA (Table DR1),¹ using natural and synthetic mineral standards.

End-member phase activities were calculated from microprobe spot analyses using AX (written and distributed by Tim Holland and Roger Powell), and P-T estimates were determined with THERMOCALC v3.21 using the February 2002 database (Powell and Holland, 1988) to either calculate intersections among well-known geothermometers and geobarometers, or, where preferred reactions were not

applicable, average intersections among all reactions (Table 2, Fig. 5).

The Devonian-Carboniferous basins are characterized by post-Caledonian low greenschist-facies metamorphism with the local development of a weak cleavage and metamorphic chlorite (Séranne and Séguret, 1987). The structurally lower Sunnarvik Group exhibits primarily Caledonian greenschist-facies assemblages defined by chlorite + muscovite + albite + quartz ± biotite ± epidote. Small, prograde-zoned garnets (≤1 mm) associated with albite + chlorite + muscovite + epidote in one gneiss from Stavøya indicate local albite-epidote-amphibolite facies conditions. Thermobarometry using all

¹GSA Data Repository item 2007209, Table DR1, electron microprobe spot analyses, and Appendix DR1, details for Sm-Nd isotopic analysis, is available at <http://www.geosociety.org/pubs/ft2007.htm> or by request to editing@geosociety.org.

TABLE 2. THERMOCALC PRESSURE-TEMPERATURE ESTIMATES FROM THE HORNELEN REGION

Sample	Unit	Thermometer [†]	Barometer [†]	Phase assemblage	T (°C)	P (kbar) [‡]	Cor. [§]
3727C	Sunnarvik	THERMOCALC: average P–T		peak	442 ± 71	9.1 ± 1.3	0.85
2801N	Lykkjebø	GARB	GBMP	peak	587 ± 63	14.9 ± 1.5	0.91
		GARB	GBM	peak	610 ± 61	19.5 ± 1.2	0.62
2803AA1	Lykkjebø	GARB	GBMP	peak	541 ± 76	14.0 ± 1.8	0.92
		GARB	GBM	peak	549 ± 72	15.8 ± 1.4	0.46
2803AA2	Lykkjebø	GARB	GBMP	peak	537 ± 78	16.4 ± 2.1	0.94
		GARB	GBM	peak	524 ± 70	13.8 ± 1.4	0.36
		GARB	GBMP	retrograde	631 ± 96	11.6 ± 1.7	0.94
2805D1	Lykkjebø	GARB	GBM	retrograde	630 ± 89	11.4 ± 1.7	0.21
		GARB	GBMP	peak	540 ± 78	15.2 ± 2.0	0.94
		GARB	GBM	peak	538 ± 72	14.7 ± 1.4	0.41
2813X	Lykkjebø	GARB	GBMP	retrograde	519 ± 72	8.5 ± 1.2	0.93
		GARB	GBM	retrograde	530 ± 68	10.7 ± 1.4	0.17
		GARB	GBMP	peak	618 ± 92	15.4 ± 2.1	0.95
		GARB	GBM	peak	629 ± 87	17.5 ± 1.6	0.55
3705A4	Lykkjebø	GARB	GBMP	retrograde	643 ± 96	10.5 ± 1.6	0.95
		GARB	GBM	retrograde	650 ± 91	11.8 ± 1.6	0.24
		GARB	GBMP	peak	607 ± 92	17.7 ± 2.4	0.95
		GARB	GBM	peak	605 ± 84	17.3 ± 1.5	0.58
2804L3	Lykkjebø	GARB	GBMP	peak	577 ± 84	15.2 ± 2.1	0.93
		GARB	GBM	peak	571 ± 77	14.0 ± 1.5	0.38
2811BC2	Lykkjebø	GARB	GBMP	peak	567 ± 82	15.3 ± 2.1	0.93
		GARB	GBM	peak	562 ± 74	14.3 ± 1.4	0.37
		GARH	GHPQ	peak	537 ± 60	13.3 ± 3.4	0.59
2815A	Eikefjord	GARB	GBMP	retrograde	557 ± 78	9.5 ± 1.3	0.94
		GARB	GBM	retrograde	561 ± 73	10.2 ± 1.5	0.10
		GARH	GHPQ	retrograde	524 ± 56	8.3 ± 1.1	0.77
2815MF	Eikefjord	GARH	GHPQ	peak	582 ± 63	18.0 ± 2.2	0.82
		GARH	GHPQ	retrograde	596 ± 63	8.9 ± 1.4	0.68
2815MM	Eikefjord	GARH	GHPQ	retrograde	628 ± 70	8.4 ± 1.3	0.73
2813V	Eikefjord	GARH	GHPQ	peak	577 ± 64	16.9 ± 2.2	0.77
2803CC	Western Gneiss Complex	GrnCpx	GrnCpxPhe	peak	682 ± 73	24.6 ± 2.1	0.57

[†]Reaction abbreviations: GARB—garnet-biotite, GBMP—garnet-biotite-muscovite-plagioclase, GBM—garnet-biotite-muscovite, GARH—garnet-hornblende, GHPQ—garnet-hornblende-plagioclase-quartz, GrnCpx—garnet-clinopyroxene, GrnCpxPhe—garnet-clinopyroxene-phengite.

[‡]Uncertainties are ±1σ.

[§]Correlation coefficient from THERMOCALC.

reactions among garnet + chlorite + muscovite + albite in the latter rock yields 9.1 ± 1.3 kbar and 442 ± 71 °C, indicating burial to ~30 km. Similar conditions were recorded by Upper Allochthon rocks on Bremangerlandet where greenschist-low amphibolite-facies fabrics defined by chlorite + mica + garnet in pelitic assemblages overprint hornfels fabrics associated with the Bremanger pluton (Kalvåg mélange of Bryhni and Lyse, 1985; Cuthbert, 1991).

In the Lykkjebø Group, upper amphibolite-facies idioblastic peak-pressure assemblages are overprinted by lower amphibolite-

greenschist-facies retrograde fabrics. This overprinting relationship is best seen in a distinctive garnet-muscovite schist found in all the structurally repeated sections of the Lykkjebø Group along the contacts with the Eikefjord Group. Characteristic albite porphyroblasts (An₀₀₋₀₅) contain inclusions of high-silica muscovite (3.2–3.3 atoms per formula unit, pfu) + high-Mg# biotite + garnet ± epidote/zoisite ± amphibole ± rutile. This peak-pressure assemblage is cut by retrograde, asymmetric shear fabrics composed of low-silica (3.1 atoms pfu) muscovite + low Mg# biotite +

garnet + oligoclase (An₁₅₋₃₀) ± chlorite ± epidote/zoisite ± ilmenite (Fig. 6). Garnets up to 5 mm in diameter in the matrix and included within albite porphyroblasts display bell-shaped Mn profiles without rim spikes and U-shaped Mg# profiles that indicate prograde growth. In retrogressed samples, increased Mg# ratios and Mn spikes in slightly resorbed garnet rims suggest heating during the initial stages of decompression (Kohn and Spear, 2000). Growth of chlorite in the foliation and along shear bands indicates that retrograde deformation within these pelites continued

through greenschist-facies conditions outside the stability field of garnet.

The P-T paths of the Lykkjebø Group pelites were calculated in THERMOCALC, using the intersection between the garnet-biotite (GARb, Ferry and Spear, 1978) thermometer and garnet-biotite-muscovite-plagioclase (GBMP, Ghent and Stout, 1981) barometer. These estimates are statistically indistinguishable from intersections between GARb and garnet-biotite-muscovite barometry (GBM, e.g., Konopasek, 1998), which do not rely upon the anorthite content of plagioclase. Mineral analyses from the albite-inclusion suite and garnet mantles in all eight samples yield peak conditions ranging from 14.0 to 17.7 kbar and 537 to 618 °C. In contrast, analyses from matrix phases and retrograde garnet rims that define top-W asymmetric shear fabrics from three of the eight samples yield metamorphic conditions ranging from 8.5 to 11.6 kbar and 519 to 641 °C.

Upper-amphibolite facies peak conditions with lower-pressure overprints are also recorded in a variety of amphibole schists in the Eikefjord Group. In plagioclase + biotite + amphibole ± muscovite schists, garnet typically forms <0.5-mm inclusions within albite, and occasionally matrix porphyroblasts up to 3 mm in diameter in more felsic layers. Garnets typically display bell-shaped Mn profiles with increasing Mg# toward rims, whereas Mn spikes near rims in many samples indicate garnet resorption. Amphibole is zoned, with sharp increases in Al content and decreases in Mg# near grain boundaries with garnet, whereas plagioclase is composed of albite overgrown by oligoclase. P-T conditions in these amphibole-bearing

rocks were calculated with THERMOCALC, using garnet-hornblende thermometry (GAHR, Graham and Powell, 1984) and garnet-hornblende-plagioclase-quartz barometry (GHPQ, Kohn and Spear, 1990). Peak conditions of 16.9–18.0 kbar at 577–582 °C were recovered from two samples using amphibole + garnet rim compositions included within albite, whereas retrograde conditions of 8.3–8.9 kbar at 524–628 °C from three samples were calculated using mineral compositions from oligoclase, garnet mantles, and amphiboles judged unaffected by late exchange reactions. There is no significant difference in the peak or retrograde pressures observed in the Eikefjord and Lykkjebø Groups, both of which indicate maximum burial depths of ~45–60 km followed by retrograde deformation at ~30–40 km depth.

The Eikefjord Group also includes lenses of coarse garnet amphibolites and rare garnet anorthosites preserved in low-strain zones. In contrast to the schists of the Lykkjebø and Eikefjord Groups, garnets from these rocks are homogenous in Mn and Mg, and Mn-rich resorbed rims are characterized by sharp decreases in Mg# that suggest cooling during retrogression. Although quantitative thermobarometric work on these rocks was precluded by textural evidence for mineral disequilibria, compositionally homogenous garnets indicate metamorphic temperatures high enough for diffusion in garnet and suggest that these rocks may be similar to relicts of Sveconorwegian granulite-facies metamorphism reported throughout western Norway in rocks correlated with the Middle Allochthon (Schärer, 1980; Corfu and Andersen, 2002).

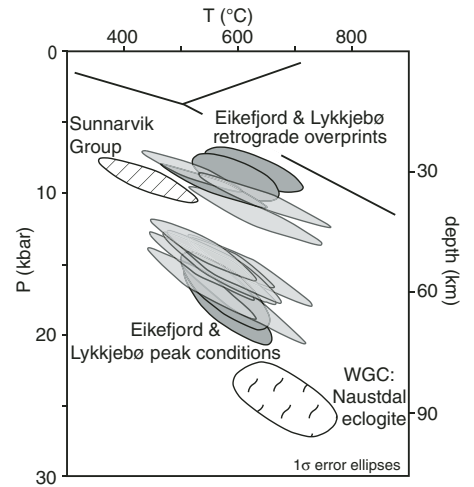


Figure 5. P-T conditions calculated from the Hornelen Region, illustrating sharp jumps in peak metamorphic conditions across tectonostratigraphic contacts and retrograde overprints in the Lykkjebø and Eikefjord Groups. Ellipse shading refers to key in Figure 2.

Structurally below the Lykkjebø and Eikefjord Groups, peak metamorphic conditions within the Western Gneiss Complex reached eclogite facies. Although the felsic host gneisses of the Western Gneiss Complex are composed of amphibolite-facies assemblages, m- to km-scale mafic boudins preserve the assemblage garnet + omphacite ± amphibole ± muscovite ± rutile (e.g., Cuthbert et al., 2000). One sample from the Naustdal eclogite

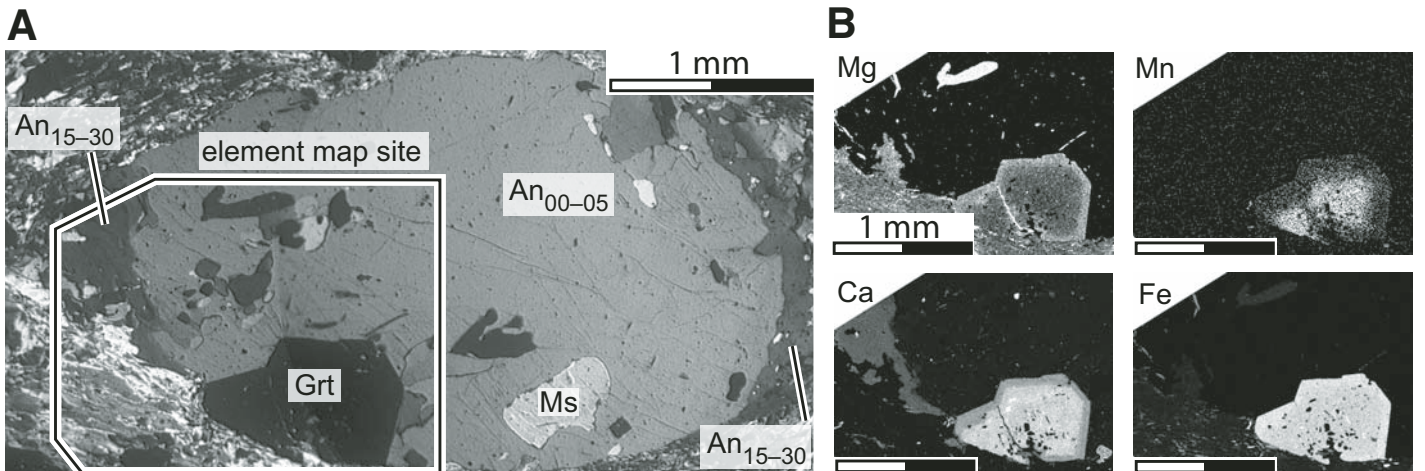


Figure 6. (A) Photomicrograph (crossed polarizers) of sample 2803AA1, showing an albite porphyroblast characteristic of the peak Lykkjebø Group assemblage cut by shear fabrics associated with top-W displacement along the Nordfjord-Sogn Detachment Zone. (B) Major-element maps (concentration scales with brightness) indicate prograde growth in garnet and oligoclase overgrowths in albite porphyroblast strain shadows.

ite contains <0.5 mm idioblastic garnets with homogeneous major element profiles, omphacite with rimward-increasing Mg#, and white mica with 3.3 Si atoms pfu. THERMOCALC intersections between garnet-clinopyroxene thermometry and garnet-omphacite-phengite barometry (see Hacker, 2006) for homogeneous garnets, low Fe/Mg omphacite cores and high Fe/Mg white mica yield 24.6 ± 2.1 kbar at 682 ± 73 °C, corresponding to a depth of ~85 km. Using the method of Stipska and Powell (2005) to estimate Fe³⁺ and the spreadsheet of Ravna and Terry (2004) yields 25 kbar at 650 ± 30 °C.

In summary, the new thermobarometry quantifies the distinct breaks in metamorphic grade between the different tectonostratigraphic units of the Hornelen Region identified by regional mapping and petrography. Whereas the Sunnarvik Group reached only greenschist-blueschist facies conditions of 9.1 ± 1.3 kbar and 442 ± 71 °C, the Eikefjord and Lykkjebø Groups reached upper-amphibolite facies conditions at 13–18 kbar and 530–620 °C, and the Western Gneiss Complex achieved eclogite-facies conditions of 24.6 ± 2.1 kbar at 682 ± 73 °C. These pressures indicate tectonic burial to ~30, 45–60, and 85 km for the Sunnarvik Group, Eikefjord and Lykkjebø Groups, and Western Gneiss Complex, respectively. This corresponds to 15–30 km of crustal excision between the Upper and Middle Allochthons, and 25–40 km of excision between the Middle Allochthon and Baltica basement. This work has also identified a high-temperature event of

probable Sveconorwegian age in the Eikefjord Group, and a Late-Caledonian event within the Eikefjord and Lykkjebø Groups associated with top-W shear fabrics at 8–12 kbar and 520–650 °C at a crustal depth of ~30–40 km.

Sm-Nd GARNET GEOCHRONOLOGY

Sm-Nd geochronology of garnet cores and rims was performed to constrain the age and duration of prograde metamorphism within the allochthons and provide an upper limit on the timing of top-W deformation within the Nordfjord-Sogn Detachment Zone. Three of the coarse garnet-muscovite schists from the Lykkjebø Group that display only minor retrograde deformation were selected for micro-sampling of garnet cores, garnet rims, and matrix (whole-rock minus garnet) fractions. To ensure that garnet core and rim fractions were accurately micro-sampled and that high-REE element inclusions in garnet were avoided, garnets were placed in epoxy grain mounts, ground down to the geometric center of the garnets, and polished for electron microscopy. Phase zoning and the relative position of garnet cores and rims were identified through compositional transects acquired with an energy-dispersive detector, and back-scattered electron imaging was used to locate high-REE element inclusions within the garnet. Micro samples of 5–14 mg were collected using a Dremel tool with a Brasseler Instruments diamond bur to scour ~1-mm-deep sample pits (inset Fig. 7A). Garnet fractions were sampled directly from

garnet mounts, and matrix fractions were sampled from unpolished thick-sections cut from hand samples. Isotopic analysis (described in detail in Appendix DR1; see footnote 1) was performed at the University of Arizona following the procedure of Ducea et al. (2003).

The Sm/Nd isotopic data yield core/rim ages of $425.1 \pm 1.6/415.0 \pm 2.3$ Ma and $422.3 \pm 1.6/407.6 \pm 1.3$ Ma for samples J2804L3 and J2805D1, respectively, and a rim age of 414.4 ± 1.6 Ma for sample J2801N (Table 3, Figure 7A, B). As indicated by thermobarometry and the presence of bell-shaped Mn profiles, these garnets never exceeded the closure temperature of >650 °C for Sm-Nd in garnet (Dodson, 1973; Van Orman et al., 2002), and core ages are therefore interpreted to represent the time of initial garnet growth, whereas rim ages represent the end of garnet growth during peak metamorphism. Because two-point isochrons cannot test for original homogeneity in ¹⁴³Nd/¹⁴⁴Nd among phases or ensure that all phases remained closed to Sm/Nd diffusion, these ages must be interpreted cautiously. Furthermore, because the core ages use a matrix composition that remained open to Sm/Nd diffusion after the closure of garnet cores, they should be regarded as minima. However, the high closure temperature of Sm/Nd diffusion and the similarities in age of the three analyzed samples suggest that a maximum age of 425–422 Ma and a rim age of 415–407 Ma represent robust ages for the onset and end of amphibolite-facies metamorphism in the Lykkjebø Group.

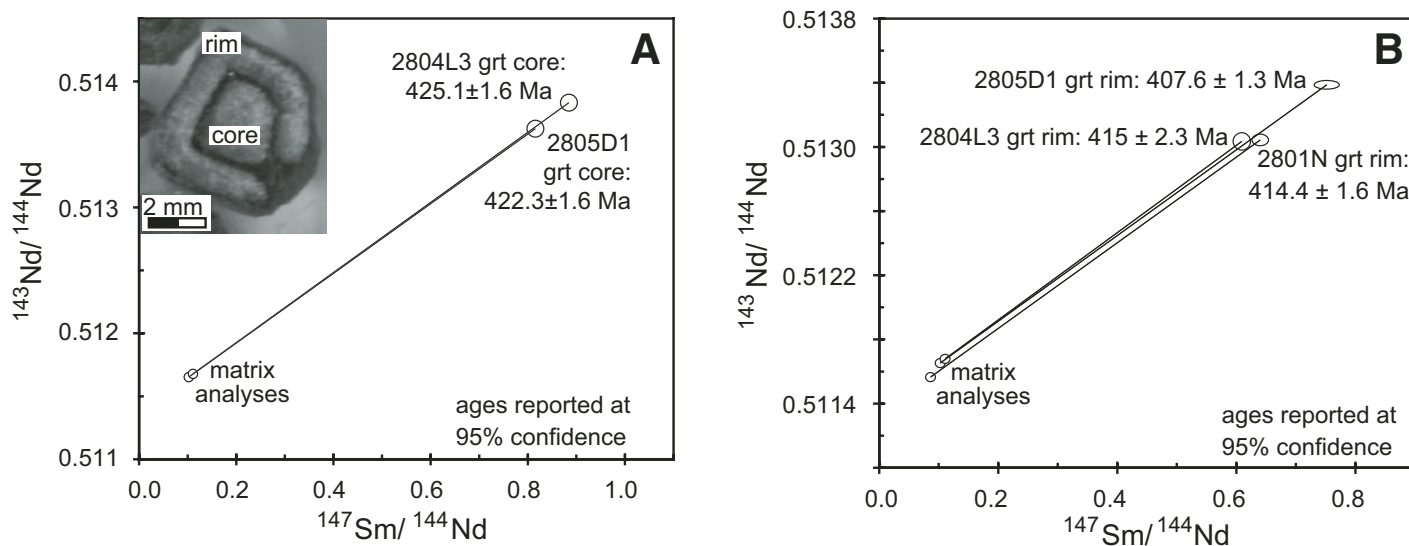


Figure 7. Sm/Nd two-point isochrons for (A) garnet cores and (B) rims from the Lykkjebø Group indicate garnet growth began at 425–422 Ma and ended by 415–407 Ma (uncertainties on individual data are smaller than shown). Inset to (A) shows a garnet from Lykkjebø Group garnet-muscovite schist 2801N mounted in epoxy and micro-sampled for cores and rims.

DISCUSSION

Strain Partitioning within the Nordfjord-Sogn Detachment Zone

The new structural data and quartz-fabric analyses place constraints on strain partitioning along tectonostratigraphic contacts and within the top-W fabrics of the Nordfjord-Sogn Detachment Zone. Consistent top-W shear-fabrics and quartz LPOs throughout the shear zone indicate that top-W displacement affected a broad shear zone focused within the Svartekari, Eikefjord, and Lykkjebø Groups, although the progressive change from subgrain-rotation recovery to grain-boundary-migration recovery observed in quartz from higher to lower structural levels across the zone indicates either downward-decreasing strain rate with constant temperature or downward-increasing strain rate with downward-increasing temperature (e.g., Stipp et al., 2002a). To assess these possibilities, strain rates across the shear zone were calculated using the flow laws of Hirth et al. (2001) with differential stresses of 48 MPa and 55 MPa determined from structurally high and low Lykkjebø Group quartz grain sizes, respectively, and f_{H_2O} at 1000 MPa confining pressure determined from retrograde barometry (Table 4). Assuming temperatures of 550 °C, structurally high Lykkjebø Group quartzites yield strain rates of $2 \times 10^{-10} s^{-1}$; investigating a range of geotherms from ~0 to 50 °C/km and temperatures of 550–600 °C, yields strain rates of $1 \times 10^{-10} - 4 \times 10^{-10} s^{-1}$ for structurally low Lykkjebø Group quartzites. The similarity between calculated strain rates in upper and lower structural levels precludes discrimination between the possible mechanisms for the downward switch from subgrain-rotation recovery to grain-boundary migration recovery. However, the data indicate that variation in strain rate was small throughout the structural stack. Measured grain sizes and calculated strain rates are comparable to observations in quartz aggregates from other extensional detachments (e.g., Hacker et al., 1990; Hacker et al., 1992). When integrated across the entire thickness of the Nordfjord-Sogn Detachment Zone, however, they yield unrealistically large shear displacements over million-year time scales. These high displacement rates may be the result of extrapolating a theoretical piezometer and experimental flow laws for pure quartzite to natural deformation of quartzofeldspathic rocks. Regardless of the absolute values of the calculated strain rates, the consistency of quartz grain sizes throughout the shear zone suggests that strain rates were relatively constant during high-temperature shear along the Nordfjord-Sogn Detachment Zone.

TABLE 3. Sm/Nd ISOTOPIC DATA FOR LYKKJEBØ GROUP GARNET-MUSCOVITE SCHISTS

Sample	Sm (ppm)	Nd (ppm)	$^{147}Sm/^{144}Nd^{\dagger}$	$^{143}Nd/^{144}Nd^{\ddagger}$	Age (Ma) [§]
2804L3 grt core	5.84	3.99	0.88464	0.513834 ± 5	425.1 ± 1.6
2804L3 grt rim	5.05	5.01	0.60923	0.513034 ± 6	415.0 ± 2.3
2804L3 matrix [¶]	4.97	27.16	0.11060	0.511679 ± 2	
2805D1 grt core	3.98	2.95	0.81543	0.513625 ± 5	422.3 ± 1.6
2805D1 rim	4.38	3.52	0.75207	0.513387 ± 2	407.6 ± 1.3
2805D1 matrix [¶]	3.99	23.54	0.10245	0.511653 ± 2	
2801N grt rim	4.43	4.18	0.64055	0.513042 ± 4	414.4 ± 1.6
2801N matrix [¶]	3.55	22.64	0.09477	0.511561 ± 1	

[†] $^{147}Sm/^{144}Nd$ errors are ~0.25%.

[‡] $^{143}Nd/^{144}Nd$ normalized to $^{146}Nd/^{144}Nd = 0.7219$ and standard errors (2 σ) refer to the last decimal place only.

[§]Because ages are derived from two-point isochrons, errors (reported at 95% confidence) are analytical only.

[¶]Matrix samples refer to whole-rock fractions sampled from the rock matrix enclosing garnet, but specifically avoiding garnet itself.

TABLE 4. QUARTZITE STRAIN RATES

Structural level	A. Strain rates in high-temperature Lykkjebø Group quartzites			
	600° C	560° C	550° C	500° C
	–log($\dot{\epsilon}$); P = 1000 ± 200 MPa [†]			
high	9.2 ± 1.1	9.7 ± 1.1	9.7 ± 1.1	10.4 ± 1.2
low	9.4 ± 1.1	9.8 ± 1.1	10.0 ± 1.2	10.6 ± 1.2
	–log($\dot{\epsilon}$); P = 1000 ± 200 MPa [†]			
high	9.3 ± 1.1	9.7 ± 1.1	9.8 ± 1.1	10.4 ± 1.2
low	9.4 ± 1.1	9.9 ± 1.1	10.0 ± 1.1	10.6 ± 1.2
Structural level	B. Strain rates in late ductile–brittle quartzite mylonites			
	400° C			300° C
	–log($\dot{\epsilon}$); P = 500 ± 100 MPa [†]			
D–B fault	11.8 ± 1.3			14.0 ± 1.5
	–log($\dot{\epsilon}$); P = 500 ± 100 MPa [†]			
D–B fault	11.8 ± 1.3			14.0 ± 1.5

Note: Strain rates calculated using the quartz flow laws of Hirth et al. (2001); one sigma errors are derived through Monte Carlo simulations propagating errors on grain size, f_{H_2O} , creep activation energy (Q), and the material constant (A); D–B fault—ductile–brittle fault.

[†] f_{H_2O} normalized to P = 1000 ± 200 MPa—the initial depth of top-W shear fabrics.

[‡] f_{H_2O} normalized to P = 500 ± 100 MPa—the probable depth of deformation during late top-W displacement along ductile–brittle detachments.

Assuming a temperature of 400 °C with f_{H_2O} normalized to 500 MPa confining pressure, the quartzites sampled from the ductile–brittle detachments deformed at significantly slower strain rates of $2 \times 10^{-12} s^{-1}$ (Table 4B). The slower strain rates and m- to dm-scale thickness suggest that the shear zones associated with these ductile–brittle detachments were only responsible for relatively minor and final stages of top-W displacement within the Nordfjord-Sogn Detachment Zone.

These results indicate that top-W strain within the Nordfjord-Sogn Detachment Zone was initially rather evenly distributed at all structural levels throughout the allochthonous nappes, and was not concentrated along the Western Gneiss Complex/allochthon contact. These data support the qualitative observation of distributed shear strain throughout the Lower and Middle allochthons by Wilks and Cuthbert (1994). During continued extension and exhumation, the

final increments of displacement within the Nordfjord-Sogn Detachment Zone were progressively focused along discrete ductile–brittle shear zones that cut the earlier high-temperature top-W fabrics.

Crustal Exhumation and the Depth of Asymmetric Shear Fabrics within the Nordfjord-Sogn Detachment Zone

The new thermobarometry quantifies total crustal exhumation across the Nordfjord-Sogn Detachment Zone and the depth at which asymmetric shear fabrics within the shear zone were initiated. Metamorphic breaks between tectonostratigraphic units in the Hornelen Region are similar to observations from the Solund Region that indicate discrete jumps in pressure from 7–9 kbar in the Upper Allochthon to 14–16 kbar in the Middle Allochthon, and finally 23 kbar in Western Gneiss Complex basement

(Hacker et al., 2003), implying the same series of orogenic events in both locations separated by 100 km. Whereas the ultimate juxtaposition of the Western Gneiss Complex with Devonian-Carboniferous sediments corresponds to cumulative crustal excision of up to 85 km across the shear zone, the 7–12 kbar jump in peak metamorphic conditions between the Western Gneiss Complex and the Lower/Middle Allochthons in the Hornelen Region—and the 7- to 9-kbar jump in the Solund Region—was overprinted by similar ~10-kbar, amphibolite-facies, asymmetric shear fabrics at both structural levels. Because the bulk of the top-W deformation within the Nordfjord-Sogn Detachment Zone occurred within the allochthonous Svartekari, Eikefjord, and Lykkjebø Groups, the depth at which these top-W fabrics initiated is constrained by the metamorphic conditions within these rocks. The retrograde assemblages of the Eikefjord and Lykkjebø Groups directly associated with top-W shear fabrics provide an estimate of 8–12 kbar for the initiation of deformation within the shear zone, whereas the relatively statically grown inclusion suite provides an upper limit of 13–18 kbar. This indicates that top-W normal-sense displacement across the Nordfjord-Sogn Detachment Zone was initiated at lower crustal depths of 30–40 km with a deeper limit of 45–60 km.

Timing of Allochthon Burial and Asymmetric Shear Fabrics within the Nordfjord-Sogn Detachment Zone

Our new garnet Sm/Nd ages have significant implications regarding the spatial variation and timing of Caledonian burial in the Middle Allochthon. Garnet core ages of 425–422 Ma coincide with the post-Wenlockian (428–423 Ma) emplacement of the Solund-Stavfjord Ophiolite (Andersen et al., 1998) and the 423–422 Ma zircon ages from eclogites in the Middle Allochthon Lindås nappe (Bingen et al., 2004), suggesting that the burial of the Middle Allochthon to depths of 45–60 km initiated during ophiolite emplacement. However, garnet rim ages of 415–407 Ma overlap with the upper range of 412–400 Ma Sm/Nd and U/Pb ages for the timing of (U)HP metamorphism north of Nordfjord (Carswell et al., 2003; Root et al., 2004; Kylander-Clark et al., 2007) indicating that this garnet growth may have been associated with the early stages of the Caledonian UHP event. In contrast, rocks of Middle Allochthon affinity in the hanging wall of the Nordfjord-Sogn Detachment Zone in the Kvamshesten area (e.g., Andersen et al., 1998; Corfu and Andersen, 2002) cooled through muscovite closure by 450 Ma and were at the surface during the deposition of the Devonian-Carboniferous Kvamshesten Basin

(Andersen et al., 1998). This suggests that rocks of Middle Allochthon affinity from different structural levels experienced drastically different Late Caledonian histories. While large tracts of the Middle Allochthon remained at or near the surface, other levels of the Middle Allochthon were (re)buried during the Late Silurian and Early Devonian. The age of 425–407 Ma for prograde garnet growth within Middle Allochthon rocks from the Hornelen Region implies that peak conditions achieved during this second episode of Middle Allochthon burial either slightly predated, or were synchronous with, subduction of the Western Gneiss Complex to UHP depths.

Garnet Sm/Nd ages can be used in conjunction with existing $^{40}\text{Ar}/^{39}\text{Ar}$ muscovite cooling ages from the Hornelen Region to place upper and lower age brackets on deformation along the Nordfjord-Sogn Detachment Zone. Because the top-W fabrics of the shear zone overprint the peak assemblage associated with garnet growth, 415- to 407-Ma garnet rim ages define an upper age limit for the initiation of top-W displacement along the shear zone. Muscovite ages are used to define the lower age limit for ductile displacement within the shear zone because the bulk of the exhumation occurred within the ductile shear fabrics of the shear zone at amphibolite-facies temperatures greater than muscovite closure to argon. Within the Hornelen Region, muscovite ages gradually increase up-section from 396 Ma in the Western Gneiss Complex to 402 Ma in the Lykkjebø Group (Andersen, 1998), whereas older ages of 419–417 Ma in the structurally highest levels of the Lykkjebø Group are the result of excess argon (Johnston et al., 2006). Together, these ages bracket top-W ductile displacement within the zone to ca. 410–400 Ma, and imply that displacement and exhumation associated with the shear zone were initiated either during, or immediately after, (U)HP metamorphism in the Western Gneiss Complex.

Significance of Normal-Sense Fabrics within the Nordfjord-Sogn Detachment Zone and a Model for UHP Exhumation

The synthesis of these quantitative results indicates that top-W displacement within the Nordfjord-Sogn Detachment Zone exhumed (U)HP rocks from the base of the crust, but not from mantle depths, and requires a new three-stage exhumation model (Fig. 8). Evidence for an initial stage of exhumation from mantle depths is provided by the abrupt jump in metamorphic pressures across the Western Gneiss Complex/allochthon contact from mantle conditions of ~25 kbar to lower crustal conditions at

13–18 kbar. However, several lines of evidence suggest that these two units were juxtaposed prior to the onset of top-W displacement within the zone. Whereas eclogite-facies asymmetric fabrics are not observed at any tectonostratigraphic level within the Nordfjord-Sogn Detachment Zone, the new thermobarometry from the Eikefjord and Lykkjebø Groups and similar amphibolite-facies asymmetric shear fabrics in the uppermost levels of the Western Gneiss Complex (e.g., Engvik and Andersen, 2000) indicates that the top-W shear fabrics of the shear zone initiated at amphibolite-facies conditions typical of lower crustal depths of 30–40 km and not at mantle depths. Furthermore, quartz microstructures that indicate relatively evenly distributed shear strain throughout the shear zone place the bulk of the top-W displacement within the Svartekari, Eikefjord, and Lykkjebø Groups. Because the bulk of the displacement within the shear zone occurred within the allochthons and not along the Western Gneiss Complex/allochthon contact, the top-W fabrics of the shear zone cannot have been responsible for the juxtaposition of the amphibolite-facies allochthons with the (U)HP Western Gneiss Complex, nor can they have been the primary mechanism responsible for exhuming the Western Gneiss Complex from mantle depths to the base of the crust. Finally, eclogites in rocks of allochthonous affinity farther north (Young et al., 2007) suggest that the observed gap in metamorphic pressures in the study area may also have been exacerbated by local phase disequilibrium in the allochthons, or poor preservation of peak pressure assemblages.

In this paper, we follow Walsh et al. (2007) and suggest that the break in metamorphic pressures across the Western Gneiss Complex/allochthon contact was created as the Western Gneiss Complex ascended buoyantly through the mantle via lower crustal-wedge extrusion and was underplated beneath the allochthons (Fig. 8B). This ascent may have been partially accommodated by localized top-W, normal-sense displacement along the Western Gneiss Complex/allochthon contact (e.g., Andersen and Jamtveit, 1990; Krabbendam and Dewey, 1998), although any fabrics associated with this displacement were overprinted by subsequent crustal exhumation. Upon arrival at the lower crust, vertical pure-shear thinning of 50–80% in the Western Gneiss Complex accommodated additional exhumation (Dewey et al., 1993; Young et al., 2007) and further exaggerated the break in metamorphic pressures between the Western Gneiss Complex and the allochthons.

The second and third stages of (U)HP exhumation—accounting for exhumation of (U)HP rocks from the lower crust to mid and upper crustal levels, respectively—were achieved

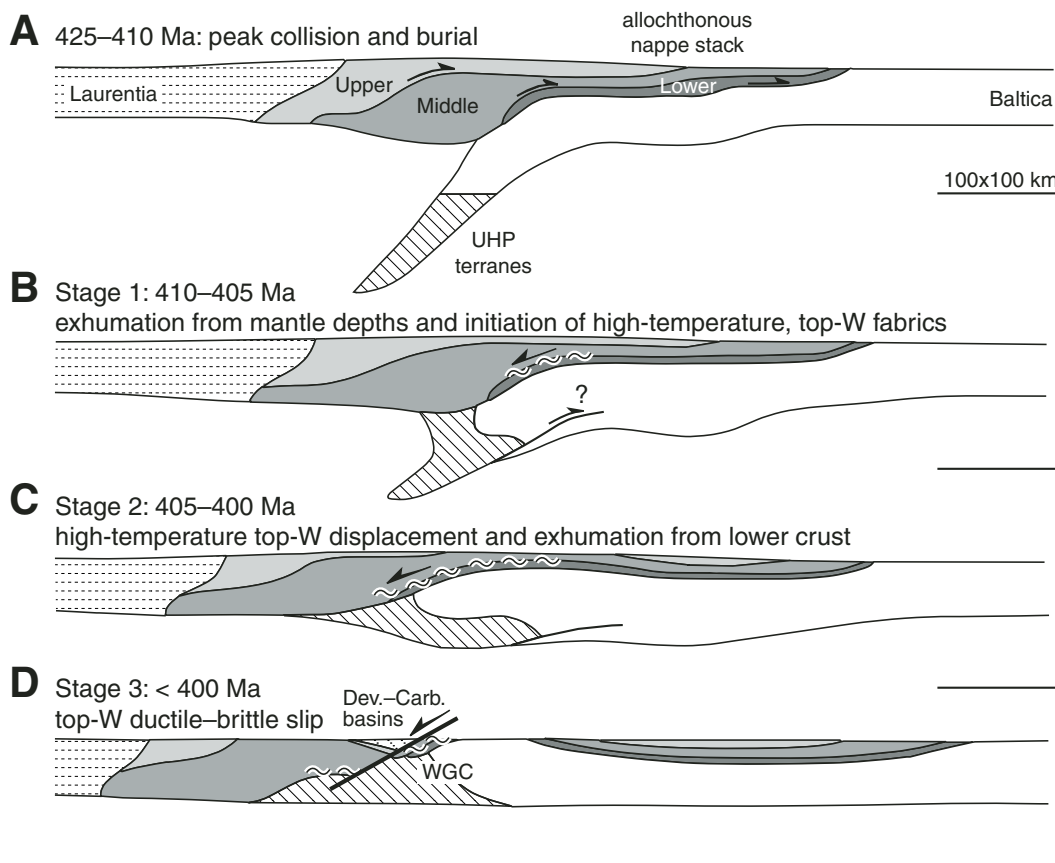


Figure 8. Schematic cross sections illustrating three individual structural regimes active within the Nordfjord-Sogn Detachment Zone that cumulatively exhumed the (U)HP provinces of western Norway. Time frames are approximate and refer only to the Hornelen Region as variations; cooling ages observed along strike of the orogen suggest subtle differences in exhumation history. (A) Geometry at the height of collision. (B) Mantle exhumation: shown here as a crustal-scale (U)HP thrust sheet rising buoyantly along the subduction zone and underplating the allochthons. Early, top-W displacement along the shear zone begins as the rising (U)HP body contacts the lower crust (shown by wavy lines). (C) Orogen-wide extension: widespread lower crustal stretching and high-temperature top-W ductile displacement within the shear zone. (D) Ductile–brittle detachment faults (shown with heavy solid line) progressively exhume and excise earlier high-temperature top-W fabrics developed within the shear zone. WGC—Western Gneiss Complex; Dev.–Carb.—Devonian–Carboniferous.

through top-W displacement within the Nordfjord-Sogn Detachment Zone. The second stage of exhumation was initiated after 410 Ma as a broad, top-W ductile shear zone centered within the allochthons formed to accommodate lower crustal reorganization and the addition of large volumes of former-(U)HP continental crust to the base of the crust (Fig. 8B, C). Although a bulk constrictional strain field during exhumation is not ruled out (Krabbendam and Dewey, 1998; Osmundsen et al., 1998; Foreman et al., 2005), quartzite LPOs indicate that plane strain conditions define Zone top-W shear fabrics. During progressive exhumation and cooling, high-temperature shear fabrics passed through muscovite closure by ca. 400 Ma, and were

cut by discrete ductile–brittle shear zones in the third and final stage of (U)HP exhumation (Fig. 8D). This three-stage model is significant in that it constrains normal-sense displacement to the component of exhumation that lifted UHP rocks from the lower to the upper crust, and underscores the importance of further work focusing on the mechanisms responsible for exhuming UHP rocks from mantle depths to the base of the crust.

CONCLUSIONS

Orogen-scale, normal-sense shear zones are commonly cited as one of the primary mechanisms responsible for the exhumation of large

UHP provinces, and the characterization of these crustal-scale detachments is essential to understanding the processes that exhume UHP rocks. Key thermobarometry geochronology, and structural geology results from the Nordfjord-Sogn Detachment Zone in western Norway indicate that (1) top-W shear within the shear zone initiated at lower crustal depths of 30–40 km; (2) top-W shear occurred between 410 Ma and 400 Ma during or immediately after UHP metamorphism; and (3) strain was partitioned relatively evenly throughout the shear zone and was not focused along tectonostratigraphic contacts. These results indicate that normal-sense displacement within the Nordfjord-Sogn Detachment Zone was

the primary mechanism responsible for post-orogenic exhumation of the Norwegian UHP provinces from the base of the crust, but not from mantle depths. This interpretation is consistent with a three-stage model for UHP exhumation that calls for crustal exhumation dominated initially by ductile, and ultimately, by ductile-brittle, normal-sense displacement and highlights the paucity of data pertaining to an initial stage of exhumation from mantle depths to the base of the crust.

ACKNOWLEDGMENTS

Thanks to Torgeir Andersen for his encouragement and for sharing his insights on Norwegian geology with us on countless field excursions; to Phil Gans and Jim Mattinson for thoughtful comments on the manuscript; and to Andrew Kylander-Clark, Emily Peterman, Matt Rioux, Dave Root, Emily Walsh, and Dave Young for countless fruitful discussions regarding Caledonian tectonics. Careful reviews and helpful comments were received from Per Terje Osmundsen and Alexander Kuehn. This work was partially funded by National Science Foundation grant EAR-0510453.

REFERENCES CITED

- Andersen, T.B., 1998, Extensional tectonics in the Caledonides of southern Norway, an overview: *Tectonophysics*, v. 285, p. 333–351, doi: 10.1016/S0040-1951(97)00277-1.
- Andersen, T.B., Berry, H.N., Lux, D.R., and Andresen, A., 1998, The tectonic significance of pre-Scandinavian $^{40}\text{Ar}/^{39}\text{Ar}$ phengite cooling ages from the Caledonides of western Norway: *Journal of the Geological Society of London*, v. 155, p. 297–309.
- Andersen, T.B., and Jamveit, B., 1990, Uplift of deep crust during orogenic extensional collapse: A model based on field studies in the Sogn-Sunnfjord region of western Norway: *Tectonics*, v. 9, p. 1097–1111.
- Andersen, T.B., Osmundsen, P.T., and Jolivet, L., 1994, Deep crustal fabrics and a model for the extensional collapse of the southwest Norwegian Caledonides: *Journal of Structural Geology*, v. 16, p. 1191–1203, doi: 10.1016/0191-8141(94)90063-9.
- Andersen, T.B., Skjerlie, K.P., and Furnes, H., 1990, The Sunnfjord Melange, evidence of Silurian ophiolite accretion in the West Norwegian Caledonides: *Journal of the Geological Society of London*, v. 147, p. 59–68.
- Baldwin, S.L., Monteleone, B.D., Webb, L.E., Fitzgerald, P.G., Grove, M., and Hill, E.J., 2004, Pliocene eclogite exhumation at plate tectonic rates in eastern Papua New Guinea: *Nature*, v. 431, p. 263–267, doi: 10.1038/nature02846.
- Beaumont, C., Jamieson, R.A., Nguyen, M.H., and Lee, B., 2001, Himalayan tectonics explained by extrusion of a low-viscosity crustal channel coupled to focused surface denudation: *Nature*, v. 414, p. 738–742, doi: 10.1038/414738a, doi: 10.1038/414738a.
- Bingen, B., Austrheim, H., Whitehouse, M.J., and Davis, W.J., 2004, Trace element signature and U-Pb geochronology of eclogite-facies zircon, Bergen Arcs, Caledonides of W Norway: *Contributions to Mineralogy and Petrology*, v. 147, p. 671–683.
- Braathen, A., 1999, Kinematics of post-Caledonian polyphase brittle faulting in the Sunnfjord region, western Norway: *Tectonophysics*, v. 302, p. 99–121, doi: 10.1016/S0040-1951(98)00281-9.
- Braathen, A., Osmundsen, P.T., and Gabrielsen, R.H., 2004, Dynamic development of fault rocks in a crustal-scale detachment; an example from western Norway: *Tectonics*, v. 23, no. 4, p. TC4010, doi: 10.1029/2003TC001558, doi: 10.1029/2003TC001558.
- Bryhni, I., 2000, Berggrunnskart NORDFJORDEID 1218 I, M 1:50,000: Foreløpig utgave Norges geologiske undersøkelse.
- Bryhni, I., and Grimstad, E., 1970, Supracrustal and infracrustal rocks in the gneiss region of the Caledonides west of Breimsvatn: *Norges Geologiske Undersøkelse*, v. 266, p. 105–140.
- Bryhni, I., and Lutro, O., 2000a, Berggrunnskart EIKEFJORD 1118 II, M 1:50,000: Foreløpig utgave Norges geologiske undersøkelse.
- Bryhni, I., and Lutro, O., 2000b, Berggrunnskart FIMLANDSGREND 1218 II, M 1:50,000: Foreløpig utgave Norges geologiske undersøkelse.
- Bryhni, I., and Lutro, O., 2000c, Berggrunnskart NAUSTDAL 1218 III, M 1:50,000: Foreløpig utgave Norges geologiske undersøkelse.
- Bryhni, I., and Lyse, K., 1985, The Kalvåg Mélange, Norwegian Caledonides, in Gee, D.G., and Sturt, B.A., eds., *The Caledonide Orogen—Scandinavia and Related Areas*: John Wiley and Sons [Chichester], p. 417–427.
- Carswell, D.A., Brueckner, H.K., Cuthbert, S.J., Mehta, K., and O'Brien, P.J., 2003, The timing of stabilisation and the exhumation rate for ultra-high pressure rocks in the Western Gneiss Region of Norway: *Journal of Metamorphic Geology*, v. 21, p. 601–612, doi: 10.1046/j.1525-1314.2003.00467.x.
- Carswell, D.A., and Cuthbert, S.J., 2003, Ultra-high pressure metamorphism in the Western Gneiss Region of Norway: *EMU Notes in Mineralogy*, v. 5, p. 51–73.
- Chauvet, A., and Séranne, M., 1994, Extension-parallel folding in the Scandinavian Caledonides: Implications for late-orogenic processes: *Tectonophysics*, v. 238, p. 31–54, doi: 10.1016/0040-1951(94)90048-5.
- Chemenda, A.I., Burg, J.-P., and Mattauer, M., 2000, Evolutionary model of the Himalaya-Tibet system: Geopem based on new modelling, geological and geophysical data: *Earth and Planetary Science Letters*, v. 174, p. 397–409, doi: 10.1016/S0012-821X(99)00277-0.
- Corfu, F., and Andersen, T.B., 2002, U-Pb ages of the Dalsfjord Complex, SW Norway, and their bearing on the correlation of allochthonous crystalline segments of the Scandinavian Caledonides: *International Journal of Earth Sciences*, v. 91, no. 6, p. 955–963, doi: 10.1007/s00531-002-0298-3.
- Cuthbert, S.J., 1991, Evolution of the Devonian Hornelen Basin, west Norway: New constraints from petrological studies of metamorphic clasts, in Morton, A.C., Todd, S.P., and Haughton, P.D.W., eds., *Developments in Sedimentary Provenance Studies*: Geological Special Publications, Geological Society, London, Special Publications, p. 343–360.
- Cuthbert, S.J., Carswell, D.A., Krogh-Ravna, E.J., and Wain, A., 2000, Eclogites and eclogites in the Western Gneiss Region: Norwegian Caledonides: *Lithos*, v. 52, p. 165–195, doi: 10.1016/S0024-4937(99)00090-0.
- Cuthbert, S.J., Harvey, M.A., and Carswell, D.A., 1983, A tectonic model for the metamorphic evolution of the Basal Gneiss Complex, Western South Norway: *Journal of Metamorphic Geology*, v. 1, p. 63–90, doi: 10.1111/j.1525-1314.1983.tb00265.x.
- Dewey, J.F., Ryan, P.D., and Andersen, T.B., 1993, Orogenic uplift and collapse, crustal thickness, fabrics and metamorphic phase changes: The role of eclogites, in Prichard, H.M., Alabaster, T., Harris, N.B.W., and Neary, C.R., eds., *Magmatic Processes and Plate Tectonics*: Geological Society, London, Special Publications, v. 76, p. 325–343.
- Dodson, M.H., 1973, Closure temperature in cooling geochronological and petrological systems: *Contributions to Mineralogy and Petrology*, v. 40, p. 259–274, doi: 10.1007/BF00373790.
- Ducea, M., Ganguly, J., Rosenberg, E.J., Patchett, P.J., Cheng, W., and Isachsen, C., 2003, Sm-Nd dating of spatially controlled domains of garnet single crystals: A new method of high-temperature chronology: *Earth and Planetary Science Letters*, v. 213, p. 31–42, doi: 10.1016/S0012-821X(03)00298-X.
- Eide, E., Haabesland, N.E., Osmundsen, P.T., Andersen, T.B., Robert, D., and Kendrick, M.A., 2005, Modern techniques and Old Red problems—determining the age of continental sedimentary deposits with $^{40}\text{Ar}/^{39}\text{Ar}$ provenance analysis in west-central Norway: *Norwegian Journal of Geology*, v. 85, p. 133–149.
- Eide, E.A., Torsvik, T.H., and Andersen, T.B., 1997, Absolute dating of brittle fault movements: Late Permian and late Jurassic extensional fault breccias in western Norway: *Terra Nova*, v. 9, p. 135–139.
- Engvik, A.K., and Andersen, T.B., 2000, Evolution of Caledonian deformation fabrics under eclogite and amphibolite facies at Vårdalsneset, Western Gneiss Region, Norway: *Journal of Metamorphic Geology*, v. 18, p. 241–257, doi: 10.1046/j.1525-1314.2000.00252.x.
- Ferry, J.M., and Spear, F.S., 1978, Experimental calibration of the partitioning of Fe and Mg between biotite and garnet: *Contributions to Mineralogy and Petrology*, v. 66, p. 113–117, doi: 10.1007/BF00372150.
- Foreman, R., Andersen, T.B., and Wheeler, J., 2005, Eclogite-facies polyphase deformation of the Drøsdal eclogite, Western Gneiss Complex, Norway, and implications for exhumation: *Tectonophysics*, v. 398, no. 1–2, p. 1–32, doi: 10.1016/j.tecto.2004.10.003.
- Fossen, H., and Dunlap, W.J., 1998, Timing and kinematics of Caledonian thrusting and extension collapse, southern Norway: evidence from $^{40}\text{Ar}/^{39}\text{Ar}$ thermochronology: *Journal of Structural Geology*, v. 20, p. 765–781, doi: 10.1016/S0191-8141(98)00007-8.
- Gee, D.G., Guezou, J.C., Roberts, D., and Wolff, F.C., 1985, The central-southern part of the Scandinavian Caledonides, in Gee, D.G., and Sturt, B.A., eds., *The Caledonide Orogen—Scandinavia and Related Areas*: John Wiley and Sons [Chichester], p. 109–133.
- Ghent, E.D., and Stout, M.Z., 1981, Geobarometry and geothermometry of plagioclase-biotite-garnet-muscovite assemblages: *Contributions to Mineralogy and Petrology*, v. 76, p. 92–97, doi: 10.1007/BF00373688.
- Glodny, J., Ring, U., Kühn, A., Gleissner, P., and Franz, G., 2005, Crystallization and very rapid exhumation of the youngest Alpine eclogites (Tauern Window, Eastern Alps) from Rb/Sr mineral assemblage analysis: *Contributions to Mineralogy and Petrology*, v. 149, p. 699–715, doi: 10.1007/s00410-005-0676-5.
- Graham, C.M., and Powell, R., 1984, A garnet-hornblende geothermometer: Calibration, testing, and application to the Pelona Schist, Southern California: *Journal of Metamorphic Geology*, v. 2, p. 13–31, doi: 10.1111/j.1525-1314.1984.tb00282.x.
- Hacker, B.R., 2006, Pressures and temperatures of ultrahigh-pressure metamorphism: Implications for UHP tectonics and H₂O in subducting slabs: *International Geology Review*, v. 48, p. 1053–1066.
- Hacker, B.R., Andersen, T.B., Root, D.B., Mehl, L., Mattinson, J.M., and Wooden, J.L., 2003, Exhumation of high-pressure rocks beneath the Solund Basin, Western Gneiss Region of Norway: *Journal of Metamorphic Geology*, v. 21, p. 613–629, doi: 10.1046/j.1525-1314.2003.00468.x.
- Hacker, B.R., and Gans, P.B., 2005, Continental collisions and the creation of ultrahigh-pressure terranes: Petrology and thermochronology of nappes in the central Scandinavian Caledonides: *Geological Society of America Bulletin*, v. 117, no. 1–2, p. 117–134, doi: 10.1130/B25549.1.
- Hacker, B.R., Yin, A., Christie, J.M., and Davis, G.A., 1992, Stress magnitude, strain rate, and rheology of extended middle crust inferred from quartz grain sizes in the Whipple Mountains, California: *Tectonics*, v. 11, p. 36–46.
- Hacker, B.R., Yin, A., Christie, J.M., and Snoke, A.W., 1990, Differential stress, strain rate, and temperatures of mylonitization in the Ruby Mountains: Implications for the rate and duration of exhumation: *Journal of Geophysical Research*, v. 95, p. 8569–8580.
- Hirth, G., Teyssier, C., and Dunlap, W.J., 2001, An evaluation of quartzite flow laws based on comparisons between experimentally and naturally deformed rocks: *International Journal of Earth Sciences*, v. 90, no. 1, p. 77–87, doi: 10.1007/s005310000152.
- Hirth, G., and Tullis, J., 1992, Dislocation creep regimes in quartz aggregates: *Journal of Structural Geology*, v. 14, no. 2, p. 145–159, doi: 10.1016/0191-8141(92)90053-Y.
- Hossack, J.R., 1984, The geometry of listric growth faults in the Devonian Basins of Sunnfjord, W. Norway: *Journal of the Geological Society of London*, v. 141, p. 629–637.
- Johnston, S., Hacker, B.R., and Andersen, T.B., 2007, Exhuming Norwegian ultrahigh-pressure rocks: Overprinting extensional structures and the role of the Nordfjord-Sogn Detachment Zone: *Tectonics* (in press).
- Johnston, S.M., 2006, Exhumation of Norwegian Ultrahigh-Pressure Rocks [Ph.D. thesis]: University of California, Santa Barbara, 132 p.

- Johnston, S.M., Hacker, B.R., Eide, E., and Hendriks, B.W.H., 2006, In situ UV-laser ablation $^{40}\text{Ar}/^{39}\text{Ar}$ muscovite thermochronology reveals excess Argon and 405–399 Ma age for the Nordfjord-Sogn Detachment Zone, Hornelen region, Norway: *Eos (Transactions, American Geophysical Union)*, v. 87, p. T41E-08.
- Johnston, S.M., Hacker, B.R., and Gehrels, G., 2003, Exhumation of Norwegian ultrahigh-pressure rocks: Zircon Geochronology and Tectonostratigraphy of the Hornelen Region: *Eos (Transactions, American Geophysical Union)*, v. 84, no. 46, p. T32F-06.
- Kohn, M.J., and Spear, F., 2000, Retrograde net transfer reaction insurance for pressure-temperature estimates: *Geology*, v. 28, p. 1127–1130, doi: 10.1130/0091-7613(2000)28<1127:RNTRIF>2.0.CO;2.
- Kohn, M.J., and Spear, F.S., 1990, Two new geobarometers for garnet amphibolites, with applications to southeastern Vermont: *American Mineralogist*, v. 75, p. 89–96.
- Konopasek, J., 1998, Formation and destabilization of the high pressure assemblage garnet-phengite-paragonite (Krusne Hory Mountains, Bohemian Massif): The significance of the Tschermak substitution in the metamorphism of pelitic rocks: *Lithos*, v. 42, no. 3–4, p. 269–284, doi: 10.1016/S0024-4937(97)00046-7.
- Krabbendam, M., and Dewey, J.F., 1998, Exhumation of UHP rocks by transtension in the Western Gneiss Region, Scandinavian Caledonides, in Holdsworth, R.E., Strachan, R.A., and Dewey, J.F., eds., *Continental Transpressional and Transtensional Tectonics*: Geological Society, London, Special Publications, p. 159–181.
- Krogh, E.J., 1977, Evidence of Precambrian continent-continent collision in Western Norway: *Nature*, v. 267, p. 17–19, doi: 10.1038/267017a0.
- Krogh, E.J., and Carswell, D.A., 1995, HP and UHP eclogites and garnet peridotites in the Scandinavian Caledonides, in Coleman, R.G., and Wang, X., eds., *Ultrahigh Pressure Metamorphism*: Cambridge University Press [Stanford], p. 244–298.
- Kylander-Clark, A., Hacker, B.R., Johnson, C.M., Beard, B.L., Mahlen, N.J., and Lapen, T.J., 2007, Coupled Lu-Hf and Sm-Nd geochronology constrains prograde and exhumation histories of high- and ultrahigh-pressure eclogites from western Norway: *Chemical Geology* (in press).
- Labrousse, L., Jolivet, L., Andersen, T.B., Agard, P., Maluski, H., and Schärer, U., 2004, Pressure-temperature-time-deformation history of the exhumation of ultra-high pressure rocks in the Western Gneiss region, Norway: *Geological Society of America Special Paper*, v. 380, p. 155–185.
- Lutro, O., and Bryhni, I., 2000, Berggrunnskart FLORØ 1118 III, M 1:50,000: Foreløpig utgave Norges geologiske undersøkelse.
- Milnes, A.G., Wennberg, O.P., Skår, Ø., and Koestler, A.G., 1997, Contraction, extension, and timing in the South Norwegian Caledonides: The Sognefjord transect, in Burg, J.-P., and Ford, M., eds., *Orogeny through Time*: Geological Society, London, Special Publications, p. 123–148.
- Norton, M.G., 1987, The Nordfjord-Sogn detachment, W. Norway: *Norsk Geologisk Tidsskrift*, v. 67, p. 93–106.
- Osmundsen, P.T., Andersen, T.B., Markussen, S., and Svendby, A.K., 1998, Tectonics and sedimentation in the hanging wall of a major extensional detachment: The Devonian Kvamshesten Basin, western Norway: *Basin Research*, v. 10, p. 213–234.
- Parrish, R.R., Gough, S.J., Searle, M., and Waters, D., 2006, Plate velocity exhumation of ultrahigh-pressure eclogites in the Pakistan Himalaya: *Geology*, v. 34, no. 11, p. 989–992, doi: 10.1130/G22796A.1, doi: 10.1130/G22796A.1.
- Powell, R., and Holland, T.J.B., 1988, An internally consistent dataset with uncertainties and correlations: 3. Applications to geobarometry, worked examples and a computer program: *Journal of Metamorphic Geology*, v. 6, p. 173–204, doi: 10.1111/j.1525-1314.1988.tb00415.x.
- Ratschbacher, L., Hacker, B.R., Calvert, A., Webb, L.E., Grimmer, J.C., McWilliams, M., Ireland, T.R., Dong, S., and Hu, J., 2003, Tectonics of the Qinling (central China): Tectonostratigraphy, geochronology, and deformation history: *Tectonophysics*, v. 366, p. 1–53, doi: 10.1016/S0040-1951(03)00053-2.
- Ratschbacher, L., Sperner, B., Meschede, M., and Frisch, W., 1994, Computer techniques and applications: A program library for quantitative structural analysis: *Tübinger Geowissenschaftliche Arbeiten*, v. 21, p. 1–73.
- Ravna, E.J.K., and Terry, M.P., 2004, Geothermobarometry of UHP and HP eclogites and schists: An evaluation of equilibria among garnet-clinopyroxene-kyanite-phengite-coesite/quartz: *Journal of Metamorphic Geology*, v. 22, no. 6, p. 579–592.
- Roberts, D., and Gee, D.G., 1985, An introduction to the structure of the Scandinavian Caledonides, in Gee, D.G., and Sturt, B.A., eds., *The Caledonide Orogen—Scandinavia and Related Areas*: John Wiley and Sons [Chichester], p. 55–68.
- Roberts, D., and Sturt, B.A., 1980, Caledonian deformation in Norway: *Journal of the Geological Society of London*, v. 137, no. 3, p. 241–250.
- Robinson, P., 1995, Extension of Trollheimen tectono-stratigraphic sequence in deep synclines near Molde and Brattvåg, Western Gneiss Region, southern Norway: *Norsk Geologisk Tidsskrift*, v. 75, p. 181–198.
- Root, D.B., Hacker, B.R., Gans, P., Eide, E., Duca, M., and Mosenfelder, J., 2005, Discrete ultrahigh-pressure domains in the Western Gneiss Region, Norway: Implications for formation and exhumation: *Journal of Metamorphic Geology*, v. 23, p. 45–61, doi: 10.1111/j.1525-1314.2005.00561.x.
- Root, D.B., Hacker, B.R., Mattinson, J.M., and Wooden, J.L., 2004, Young age and rapid exhumation of Norwegian ultrahigh-pressure rocks: An ion microprobe and chemical abrasion study: *Earth and Planetary Science Letters*, v. 228, p. 325–341, doi: 10.1016/j.epsl.2004.10.019.
- Schärer, U., 1980, U-Pb and Rb-Sr dating of a polymetamorphic nappe terrain: the Caledonian Jotun Nappe, southern Norway: *Earth and Planetary Science Letters*, v. 49, p. 205–218, doi: 10.1016/0012-821X(80)90065-5.
- Schmid, S.M., and Casey, M., 1986, Complete fabric analysis of some commonly observed quartz c-axis patterns: *Geophysical Monograph*, v. 36, p. 263–286.
- Séranne, M., and Séguret, M., 1987, The Devonian basins of western Norway: Tectonics and kinematics of extending crust: *Geological Society of London Special Publication*, v. 28, p. 537–548.
- Smith, D.C., 1984, Coesite in clinopyroxene in the Caledonides and its implications for geodynamics: *Nature*, v. 310, p. 641–644, doi: 10.1038/310641a0.
- Steel, R.J., Siedlicka, A., and Roberts, D., 1985, The Old Red Sandstone basins of Norway and their deformation: a review, in Gee, D. G., and Sturt, B. A., eds., *The Caledonide Orogen—Scandinavia and Related Areas*: John Wiley and Sons [Chichester], p. 293–316.
- Stipp, M., Stuenitz, H., Heilbronner, R., and Schmid, S.M., 2002a, Dynamic recrystallization of quartz: correlation between natural and experimental conditions: *Geological Society, London, Special Publications*, v. 200, p. 171–190.
- Stipp, M., Stuenitz, H., Heilbronner, R., and Schmid, S.M., 2002b, The eastern Tonale fault zone: a “natural laboratory” for crystal plastic deformation of quartz over a temperature range from 250 to 700 degrees C: *Journal of Structural Geology*, v. 24, no. 12, p. 1861–1884, doi: 10.1016/S0191-8141(02)00035-4.
- Stipska, P., and Powell, R., 2005, Constraining the P-T path of a MORB-type eclogite using pseudosections, garnet zoning and garnet-clinopyroxene thermometry: an example from the Bohemian Massif: *Journal of Metamorphic Geology*, v. 23, no. 8, p. 725–743, doi: 10.1111/j.1525-1314.2005.00607.x.
- Terry, M.P., Robinson, P., Hamilton, M.A., and Jercinovic, M.J., 2000, Monazite geochronology of UHP and HP metamorphism, deformation, and exhumation, Nordøyane, Western Gneiss Region, Norway: *American Mineralogist*, v. 85, p. 1651–1664.
- Torsvik, T.H., Sturt, B.A., Swenson, E., Andersen, T.B., and Dewey, J.F., 1992, Palaeomagnetic dating of fault rocks: Evidence for Permian and Mesozoic movements along the Dalsfjord Fault, Western Norway: *Geophysical Journal International*, v. 109, p. 565–580, doi: 10.1111/j.1365-246X.1992.tb00118.x.
- Twiss, R.J., 1977, Theory and applicability of a recrystallized grain size paleopiezometer: *Pure and Applied Geophysics*, v. 115, p. 227–244, doi: 10.1007/BF01637105.
- Twiss, R.J., 1980, Static theory of size variation with stress for subgrains and dynamically recrystallized grains: *U.S. Geological Survey Open-File Report*, no. 80-625, p. 665–683.
- Van Orman, J.A., Grove, T.L., Shimizu, N., and Layne, G., 2002, Rare earth element diffusion in a natural pyrope single crystal at 2.8 GPa: Contributions to Mineralogy and Petrology, v. 142, p. 416–424.
- Wain, A., 1997, New evidence for coesite in eclogite and gneisses; defining an ultrahigh-pressure province in the Western Gneiss region of Norway: *Geology*, v. 25, p. 927–930, doi: 10.1130/0091-7613(1997)025<0927:NEFCIE>2.3.CO;2.
- Walsh, E.O., and Hacker, B.R., 2004, The fate of subducted continental margins: Two-stage exhumation of the high-pressure to ultrahigh-pressure Western Gneiss complex, Norway: *Journal of Metamorphic Geology*, v. 22, p. 671–689, doi: 10.1111/j.1525-1314.2004.00541.x.
- Walsh, E.O., Hacker, B.R., Gans, P., Grove, M., and Gehrels, G., 2007, Protolith ages and exhumation histories of (ultra)high-pressure rocks across the Western Gneiss Region, Norway: *Geological Society of America Bulletin*, v. 119, no. 3/4, p. 289–301, doi: 10.1130/B25817.1, doi: 10.1130/B25817.1.
- Wilks, S.J., and Cuthbert, S.J., 1994, The evolution of the Hornelen Basin detachment system, western Norway: Implications for the style of late orogenic extension in the southern Scandinavian Caledonides: *Tectonophysics*, v. 238, p. 1–30, doi: 10.1016/0040-1951(94)90047-7.
- Young, D., 2005, Amphibolite to Ultrahigh-Pressure Transition in Western Norway [Ph.D. thesis]: University of California, Santa Barbara. 120 p.
- Young, D.J., Hacker, B.R., Andersen, T.B., and Corfu, F., 2007, Prograde amphibolite facies to ultrahigh-pressure transition along Nordfjord: Implications for exhumation tectonics: *Tectonics*, v. 26, p. TC1007, doi: 10.1029/2004TC001781, doi: 10.1029/2004TC001781.

MANUSCRIPT RECEIVED 2 JANUARY 2007

REVISED MANUSCRIPT RECEIVED 16 MAY 2007

MANUSCRIPT ACCEPTED 31 MAY 2007

Printed in the USA